Journal of Geophysical Research
NOVEMBER 2007, VOLUME 112 (B11102) : 1-18
http://dx.doi.org/10.1029/2007JB005093

Crustal structure of the basin and ridge system west of New Caledonia (Southwest Pacific) from wide-angle and reflection seismic data.

F. Klingelhoefer[1, *], Y. Lafoy[2], J. Collot[1], E. Cosquer[1], L. Géli[1], H. Nouzé[1], R. Vially[3]

[1]Dep. of Geodynamics and Geophysics, IFREMER, Centre de Brest, B.P. 70, 29280 Plouzané, France.
[2]Bureau of Geology and Mines, Department of Industry, Mines and Energy of New Caledonia, B.P. 465-98845, Nouméa, New Caledonia
[3]IFP, 1 & 4, avenue de Bois-Preau 92852 Rueil-Malmaison Cedex, France

*: Corresponding author : F. Klingelhoefer, email address : fklingel@ifremer.fr

Abstract:

During the Zoneco 11 marine geophysical survey (September 2004), two deep reflection seismic profiles recorded by ocean bottom seismometers were acquired in the offshore domain west of New Caledonia. The northern profile crosses the New Caledonia Basin, the Fairway Ridge, the Fairway Basin, and the Lord Howe Rise. The southern profile crosses the Norfolk Rise south of New Caledonia, the New Caledonia Basin, the Fairway Ridge and Basin, and ends at the foot of Lord Howe Rise. On the northern profile the Lord Howe Rise has a crustal thickness of 23 km and exhibits seismic velocities and velocity gradients characteristic of continental crust. The crust thins to 12–15 km in the neighboring Fairway Basin, which is interpreted to be of thinned continental origin based on the seismic velocities. The crustal thickness of the Fairway Rise is 22 km, and it is also interpreted to be of continental origin. The New Caledonian Basin is underlain by crust of 10 km thickness, which shows unusally high velocities (between 7.0 and 7.4) uncharacteristic for either thinned continental or oceanic crust. On the southern profile the Norfolk Rise is also found to be of continental nature. Here, the New Caledonia Basin shows velocities, crustal thickness, and basement roughness characteristic of typical oceanic crust. The crust in the Fairway Basin shows higher velocities than on the northern profile, which could be caused by volcanic intrusions into the crust during extension. A deep reflector in the upper mantle was imaged underneath the New Caledonian Basin on the northern profile.

Keywords: wide-angle seismic; SW Pacific; crustal structure.

1. Introduction and previous work

The geodynamic history of the Southwest Pacific since the Cretaceous has been characterized by the fragmentation of Gondwanaland. During an extensional period from late Cretaceous to early Eocene three subparallel marginal basins were created, the Tasman Sea, the New Caledonia Basin and the Loyalty Basin (Figure 1) separated by two aseismic ridges, Lord Howe Rise and the New Caledonia-Norfolk Ridge [*Dubois et al.*, 1974; *Ravenne et al.*, 1977; *Willcox et al.*, 1980; *Eade*, 1988; *Symonds et al.*, 1996; *Gaina et al.*, 1998; *Willcox et al.*, 2001; *Crawford et al.*, 2003; *Exon et al.*, 2004; *Lafoy et al.*, 2005a; *Pelletier*, 2006]. This opening was followed by a compressional phase in the late Eocene/early Oligocene at the end of which ophiolites were obducted onto New Caledonia and Lord Howe Rise became eroded subaerially [*Avias*, 1967; *Paris*, 1979; *Collot et al.*, 1987; *Aitchison et al.*, 1995; *Cluzel et al.*, 2001; *Exon et al.*, 2007].

Deep crustal data are generally scarce in this area. During one of the first wide-angle seismic studies carried out in the Melanesian islands area, two seismic profiles were acquired crossing the Lord Howe Rise and the New Caledonia Basin [*Shor et al.*, 1971]. From modelling of the expanding-spread profiles acquired during the cruise, the authors concluded that the Lord Howe Rise is underlain by 18 to 25 km thick continental crust and the Norfolk Ridge by 21 km thick crust. Woodward and Hunt [1971] determined the crustal structure across the Tasman Sea from gravity measurements interpreted together with the first deep seismic results from Shor et al., [1971] . They confirmed the continental nature of Lord Howe Rise and proposed volcanic intrusions to explain short wavelength gravity anomalies. They obtained a 9 km thick crust in the New Caledonia Basin from gravity modelling.

During the Sonne SO-36 cruise, magnetic and gravimetric data were acquired on the Lord Howe Rise and Dampier Ridge and in the Lord Howe Basin [*Schreckenberger et al.*, 1992]. On the basis of modelling of magnetic data the authors concluded that continental crust with a highly magnetized lower crust and slightly less magnetized upper crust provides a better fit to the data than does a model with oceanic crust.

A major compressive phase during the upper Eocene and Middle Oligocene has been proposed from DSDP drilling and seismic profiling [*Burns et al.*, 1973]. This lead to the subaerial exposure of the Lord Howe Rise and created a regional erosional unconformity. This erosion is contemporaneous with the obduction of the ophiolite onto New Caledonia. A volcanic event associated with the post Oligocene subsidence of the area is identified on the basis of imagery and seismic data [*de Beuque et al.*, 1998; *Exon et al.*, 2004]. The authors confirmed the intermediate (continental intruded by volcanism) nature of the Lord Howe Rise and proposed on the basis of the magnetic lineations, an oceanic origin of the Fairway Ridge and Basin.

The *Austradec I* and *II* marine seismic surveys were the first to discover the Fairway Ridge, a major structural feature which divides the New Caledonian (NC) basin into the NC basin *senso stricto* and the Fairway Basin. they also found, that it plays an important role as a barrier in the distribution of sediments [*Ravenne et al.*, 1977]. The Fairway ridge, previously interpreted as a ridge of oceanic nature [*Ravenne et al.*, 1977; *Mignot*, 1984] and as an oceanic piece of the New Caledonia basin crust overthrust along the Lord How Rise [*Lafoy et al.*, 1994; *de Beuque*, 1999; *Auzende et al.*, 2000] is now considered to be thinned continental crust [*Vially et al.*, 2003; *Lafoy et al.*, 2005b]. The origin of the Fairway Basin remains controversial to this day. Mignot [1984], Eade [1988], Uruski and Wood [1991], van de Beuque [1999] and Auzende et al [2000] interpreted the substratum of Fairway Basin as oceanic in nature.

The Moho depth underneath the south New Caledonia Basin has been found to be slightly deeper than priviously thought from expanded spread profiles [*Shor et al.*, 1971]. The sub-seafloor basement depth of the New Caledonia Basin was found to increase towards the west, from 2 km near Lord Howe Rise to 3 km near the Norfolk Ridge [*Woodward and Hunt*, 1971]. Origin of the basin is controversial from oceanic type [*Shor et al.*, 1971; *Dubois et al.*, 1974; *Weissel and Hayes*, 1977; *Willcox et al.*, 1980; *Kroenke*, 1984; *Mignot*, 1984; *Sutherland*, 1999; *Auzende et al.*, 2000] to thinned continental type [*Etheridge et al.*, 1989; *Uruski and Wood*, 1991; *Sdrolias et al.*, 2003; *Vially et al.*, 2003].

The western margin of New Caledonia was previously interpreted as a subduction zone active before the late Eocene and the emplacement of the New Caledonia ophiolite [*Dubois et al.*, 1974; *Kroenke*, 1984; *Collot et al.*, 1987]. In 1987 during the ZOE 400 cruise the margin was investigated by 14 seismic profiles [*Rigolot and Pelletier*, 1988]. The compressional sedimentary structures observed have been interpreted as representing a zone of deformation active between the Eocene compressional phase and the Upper Miocene or Piocene, and as having formed in response during the obduction of the peridotites on New Caledonia, which never attained full subdcution [*Rigolot and Pelletier*, 1988].

This would therefore also explain the absence of a fully developed volcanic arc on the New Caledonia island [*Rigolot and Pelletier*, 1988]. The presence of a fully developed short-lived subduction zone west of New Caledonia could also be indicated by the presence of some magmas related to an active margin found on the island [*Cluzel et al.*, 2001; *Collot et al.*, 1987].

From modelling of the source-receiver functions of 15 large earthquakes from a land station in Noumea Regnier [1988] constructed a simplified model of the crustal and mantle structure beneath southern New Caledonia. The final velocity-depth function shows a Moho depth of 26 +- 1 km. Two low velocity zones are observed in the mantle underneath Noumea, the first between 40 and 50 km depth and the second from 60 to 65 km depth. The second low velocity zone dips towards the North. Due to the absence of a volcanic arc on the island, the authors offer as the most plausible explanation that the two low velocity zones result from west coast underthrusting, which perhaps reached the early stages of subduction, with a contemporaneous east coast obduction of the ophiolite nappe.

The main aim of the deep reflection and wide-angle seismic profiling performed during the Zoneco 11 cruise in the basin and ridge region system west of New Caledonia was the determination of the crustal structure in the region of the New Caledonia Basin, the Fairway Ridge and the Fairway Basin. These geophysical data provide a new basis for reconstructing the geological history of the region.

2. Data acquisition and quality

During the Zoneco 11 cruise in 2004 two combined wide-angle and reflection seismic profiles of 500 km length each were shot across the basin and ridge region system west of New Caledonia. The seismic Profile N (Figure 1) is located around 23^o S, starting from the coast off New Caledonia and crossing the New Caledonia Basin, the Fairway Ridge, the Fairway Basin and the Lord Howe Rise and has a total length of 565 km. It was shot in two parts, with all 15 available ocean-bottom seismometers (OBS) deployed on both parts, offering a dense coverage of 10 nm between instruments. All OBS except OBS 20, in which the hard disk failed, provided useful data. Four landstations where installed on the mainland by the IRD (Institut de Recherche pour le Developpement) in the extension of the profile, of which one gave useful data. A total of 3923 shots were fired on the profile by a 8530 in^3 airgun array tuned to single-bubble mode to enhance the low frequencies and allow deep penetration [*Avedik et al.*, 1993]. The second deep seismic profile (Profile S) is located around 25^o S (Figure 1) and has a length of 538 km. It crosses the Norfolk Ridge, the New Caledonia Basin, the southern extension of the Fairway Ridge, the Fairway Basin and ends on the Lord Howe Rise. The profile was shot in two parts the first part using 15 OBS and the second 12 OBS. All OBS provided useful data, except OBS50, which could not be recovered. A total of 3922 shots were fired on this profile using the same airgun array as on Profile N. Multichannel seismic (MCS) data were acquired along the profiles using a 4.5 km long, 360 channel digital streamer.

Processing of the multichannel seismic data was performed using the Geovecteur processing package. It included spherical divergence correction, FK-filtering, bandpass filtering (3-5-50-60 Hz), internal mute and dynamic corrections. Velocity analysis was performed every 200 CDP for the final stack. The last processing step included applying an automatic gain control and a Kirchoff time migration. The sedimentary layers are well imaged in the reflection seismic section and the acoustic basement reflector is clearly distinguishable throughout the profiles. Clear reflections from the Moho are found in the New Caledonia Basin and other regions.

On both profiles, additional gravimetric data were acquired using a BGM5 gravimeter, which offers a precision between 0.4 and 1.6 mGal depending on the state of the sea, and an instrument drift less than 2 mGal per month. The data were corrected for the instrument drift and the Eötvös correction was applied to allow the calculation of the free-air anomaly. A SeaSpy proton magnetometer towed behind the seismic streamer at a depth of 6 m was used for magnetic data acquisition. Its precision is about 0.2 gamma.

Preprocessing of the OBS data included calculation of the clock-drift corrections to adjust the clock in each instrument to the GPS base time. The individual time drifts were between 0.4 and 8.2 ms per day with a mean of 2.46 ms. Instrument locations were corrected for drift from the deployment position during their descent to the seafloor using the direct water wave arrival. The drift of the instruments never exceeded 200 m.

Picking of the onset of first and secondary arrivals was performed without filtering where possible (mostly between offsets of 0 - 40 km). Different filters were applied to the instruments where necessary, depending on the quality of the data and the offset to the source. Arrivals from longer offsets are of lower frequency compared to short offset arrivals, so the filter frequencies were chosen correspondingly. On some instruments with a higher noise level, a narrow filter was used to pick arrivals from longer offsets.

Data quality on Profile N is generally very good on all four channels. On the Lord Howe Rise and Fairway Ridge useful data were recorded at offsets between the ship and the instrument of up to 200 km. OBS sections from the New Caledonia basin show several arrivals from sedimentary layers with high amplitudes (Figure 2). The crustal arrivals show one phase only with a velocity around 7 km/s. Clear high amplitude arrivals from the reflection on the Moho and slightly lower amplitude arrivals from turning rays in the upper mantle are visible on most sections from the basin. A deep reflected arrival from the upper mantle is observed underneath the New Caledonia basin (Figure 2). Arrivals from OBS sections from the Fairway Ridge and Lord Howe Rise include fewer sedimentary phases and high amplitude crustal arrivals with velocities between 6 and 6.8 km/s. Reflected arrivals from the Moho and turning rays from the upper mantle arrive later than in the New Caledonian basin indicating a larger crustal thickness (Figure 3). Data from the Fairway Basin show several sedimentary arrivals, crustal arrivals at a velocity between 6-6.8 km/s, as well as reflections from the Moho (Figure 4).

Along Profile S the data quality is equally high as along Profile N. Late P_mP and P_n arrivals underneath the Norfolk Ridge indicate a large crustal thickness (Figure 5). OBS sections from the New Caledonia Basin show high amplitude crustal arrivals (Figure 6). The crossover distance between crustal and upper mantle arrivals is about 35 km, which is typical for oceanic crust. Finally, OBS sections from Lord Howe Rise show similar characteristics as those from the northern part of the Rise, including crustal arrivals at a velocity between 6.4 and 6.8 km/s and late reflections from the Moho indicating high crustal thickness (Figure 7).

3. Velocity modelling

The data were modelled using a two-dimensional iterative damped least-squares travel-time inversion from the RAYINVR software [*Zelt and Smith*, 1992]. Modelling was performed using a layer-stripping approach, proceeding from the top of the structure towards the bottom. We used a two-dimensional iterative damped least-squares inversion of travel times [*Zelt and Smith*, 1992]. Upper layers, where not directly constrained by arrivals from within the layer, were adjusted to improve the fit of lower layers. For the model parameterization we used the minimum-parameter/minimum structure approach, to avoid inclusion of velocity or strucural features into the model unconstrained by the data [*Zelt*, 1999]. Lateral velocity changes are included into the model only if required by the data, and layers are only included if reflected arrivals or changes in the velocity gradients are necessary to explain all arrivals. Arrival times of the main sedimentary layers and basement were picked from the reflection seismic data. These were converted to depth using the OBS data and seismic velocities from velocity analysis of the reflection seismic data. The depth and velocities of the crustal layers and the upper mantle were modelled from the OBS data only. Velocity gradients and the phase identification in the velocity model were further constrained by synthetic seismogram modelling using the finite-difference modelling code from the Seismic Unix package [*Cohen and Stockwell*, 2003; *Stockwell*, 1999].

Picking uncertainties for each phase were defined by the ratio of the amplitudes 250 ms before and after onset of the picked arrival. A mean error was calculated for each phase of each station and then converted to predicted travel-time picking errors between 20 and 125 ms using the table of [*Zelt*, 1999]. Using this procedure the final χ^2 travel-time error of all modelled travel-time picks should be close to 1.0, ensuring a good quality of the fit of the model and without over interpretation of arrivals on traces with a low signal to noise ratio. All arrivals on the landstation data were assigned a picking error of 125 ms, to take into account the unreversed nature of the shots on land and the data quality. The number of picks, RMS traveltime residual and the χ^2 -error for all phases are listed in Tables 1 and 2.

The Profile N velocity model comprises 8 layers: the water layer, four sedimentary layers, two crustal layers and the upper mantle layer (Figure 8). Each layer is defined by depth and velocity nodes. Water velocity is a constant 1500 m/s throughout the model.

Seafloor bathymetry was determined from the echosounder logs. The seafloor model layer includes depth nodes at a spacing of 1.5 km (Figure 8). The sedimentary layers are modelled using the reflection seismic data for layer geometry converted to depth using velocities from the OBS data and sampled at the the same node spacing as the seafloor layer. Sediment velocities range from 2.15 m/s - 2.70 m/s, 2.80 - 3.15 km/s, 3.20 - 4.60 km/s and 5.40 - 5.50 kms. The crust was modelled by two layers of 6.4 - 6.6 km/s and 6.6 - 7.0 km/s. The top of the basement was modelled with a spacing of 8 km, as it is not well resolved in the reflection seismic data, due to the relatively small velocity increase between this layer and the overlying acoustic basement. The mid-crustal layer, the top of the underplate layer and the Moho are imaged with a lower resolution, and a depth node spacing of 10 - 12 km was adequate. The mantle velocity was set to gradient 8.00 km/s at the top of the layer and 8.40 km/s at the bottom of the model. A deep reflection from the upper mantle is modelled as a floating reflector with no associated velocity increase.

The velocity model of Profile S includes 7 layers: the water layer, three sedimentary layers, with velocities of 2.16 - 3.20 km/s, 3.20 - 4.30 km/s and 5.40 - 5.70 km/s, two crustal layers with velocities between 6.40 - 6.60 km/s and 6.60 - 7.25 km/s (Figure 9). As for Profile N the geometry of the sedimentary layers is taken from the reflection seismic profiles and converted to depth using the interval velocities calculated from the OBS data. Node spacing is the same as in Profile N: 1.5 km for the seafloor and sedimentary layers, 5 and 10 km for the basement and crustal layers.

4. Error analysis

Two-point ray-tracing between source and receiver (Figure 10) shows the well-resolved and the unconstrained areas. Ray coverage is generally very good on both profiles due to the excellent data quality. On Profile N the upper two sedimentary layers are well resolved throughout the model. The third sedimentary layer is not well sampled between 0 and 150 km model distance. Basement and crustal layers are well resolved throughout the model except in the area of New Caledonia. The Moho is well constrained by reflections and by turning rays into the upper mantle. The reflector in the mantle is well defined between 400 and 550 km model distance. All sedimentary layers are well sampled by reflected and turning waves rays in the Profile S (Figure 10). The crustal layers are well sampled except for the lower crustal layer at model distances of less than 100 km. As for Profile N, the Moho is well constrained throughout the model by reflections and turning waves. On both profiles, the Moho has been additionally constrained by gravity modelling at the ends of the profiles.

Additional information about the quality of the velocity model is offered by the resolution parameter (see Figure 11) [*Zelt and Smith*, 1992]. Resolution is a measure of the number of rays passing through a region of the model constrained by a particular velocity node and is therefore dependent on the node spacing. Nodes with values greater than 0.5, corresponding to white and light grey areas in the model, are considered well resolved (Figure 11). Only few regions of Profile N show a resolution less than 0.5. First, the crust beneath New Caledonia is not well resolved as the landstations did not yield high quality data. Second, the deeper sedimentary layers are less well resolved than the rest of the model as only few turning rays from these layers could be picked. On profile S no region with a resolution parameter value less than 0.5 can be discerned. The deeper sedimentary layers and the acoustic basement in the Fairway Basin show slightly reduced resolution values, as only few arrivals could be modelled for these layers.

The fit between predicted arrival times and travel-time picks provides information about the quality of the model (Figure 10). The χ^2 is defined as the root-mean-square traveltime misfit between observed and calculated arrivals normalised to the picking uncertainty. The number of picks, the picking error, the values for the χ^2 parameter and the rms misfit for the most important phases of the models are listed in Tables 1 and 2.

In order to estimate the velocity and depth uncertainty of the final velocity model a perturbation analysis was performed. The depth of the key interfaces was varied and an F-test was applied to determine if a significant change between the models could be detected. The 95% confidence limit gives an estimate of the depth uncertainty of the interface (see Figure 11). On Profile N the Moho is resolved to 0.5 and -0.4 km depth and the mid-crustal reflector to +0.3 and -0.5 km. Depth constraints on the basement are between +0.04 and -0.1 km. The Moho is less well constrained on the margin-parallel profiles, between 0.4 and 0.7 km. For all other interfaces the reflection seismic data additionally constrain the geometry of the reflectors, and thus the F-test does not predict a realistic value. On Profile S the Moho is constrained to +0.6 and -0.3 km, the mid crustal reflector to +0.8 and -0.3 km and finally the basement to +0.2 and -0.2 km.

5. Gravity modelling

Gravity anomalies in the study region show a close correlation of gravity highs with the ridges and lows with the basins with the lowest values found southwest of New Caledonia in the New Caledonian Basin (Figure 12). Since seismic velocities and known densities for oceanic crust are well-correlated, gravity modelling provides an important additional constraint on the seismic model. Areas unconstrained by the seismic data can be modelled by comparing calculated gravity anomalies with those observed. Average P-wave velocities for each layer of the seismic models were converted to densities using the relationship of Christensen and Mooney [1995] for crustal layers and that of Ludwig, Nafe and Drake [1970] for sedimentary layers. Upper mantle densities were set to a constant 3.32 g/cm^3. The lower crustal layer was divided into 3 regions on Profile N, of which the middle region underneath the New Caledonian Basin is characterized by slightly higher densities of 3.05 g/cm^3 (Figure 13) as compared to 2.84 g/cm^3 along the rest of the profile. The density of the lower crust on Profile S was divided into 5 regions of which the crust underneath the Fairway Basin and New Caledonia Basin have higher densities around 2.91 g/cm^3 as compared to the densities underneath the rises (Figure 13) corresponding to the higher seismic velocities found in those the basins.

The gravity data were forward modelled using the gravity module of the software of Zelt and Smith (1992). To avoid edge effects both models were extended by 100 km at both ends and down to a depth of 95 km. The calculated anomalies can be compared with the shipboard measured gravity anomaly (Figure 13). The predicted anomalies generally fit the observed data well. The largest misfit on Profile N is observed at around 225 km model distance and might be caused by three-dimensional effects of the basement topography. The largest misfits on Profile S are located on both profile ends where the seismic constraints are weaker. An additional misfit around 450 km model offset is probably due to 3-D effects, as indicated by the positive gravity anomaly in the vicinity of the profile close to the location of OBS 36 (Figure 12).

6. Comparison to reflection seismic data

The wide-angle seismic models converted to two-way travel-time show good agreement with the reflection seismic section (Figures 14 (A) and (B)). The most prominent sedimentary reflectors were taken from Lafoy and Ship. Sci. Party [2004] with slight adjustments where necessary to fit the OBS data. However, only sedimentary reflectors discernible in the OBS data and therefore necessary for the modelling were included to avoid over-parametrization of the inversion. Velocities of these main sedimentary layers were constrained by wide-angle seismic data, but some additional layering is imaged by the reflection seismics. Depth of the acoustic basement is in very good agreement along the complete model.

On Profile N the first sedimentary layer incorporated into the velocity model corresponds to the sequence from Mid-Miocene to present (Figure 14 (A)). The second layer comprises the Lower Miocene to post Upper Eocene sequences [*Lafoy and Ship. Sci. Party*, 2004]. The base of this layer is marked by a regional unconformity which was related to the obduction of the ophiolites onto New Caledonia and the corresponding compressional phase. The third sedimentary layer corresponds to the Cretaceous to Paleocene sequences. Lastly the fourth layer represents the acoustic basement. The reflection seismic data show two different facies, the first one diffractive and interpreted to be intrusive, and the second one reflective with possibly sedimentary structures. This facies could be interpreted as series from an ancient volcanic arc metamorphosed during the Rangitata orogeny in the Upper Jurassic or Lower Cretaceous [*Lafoy and Ship. Sci. Party*, 2004].

On Profile S only two instead of three sedimentary layers were included into the final velocity model (Figure 14 (B)). The first layer corresponds to the Miocene to present series and the second to the Cretaceous to Miocene series. In the New Caledonian Basin the acoustic basement shows a very diffractive facies and might correspond to the top of the oceanic crust. The Moho discontinuity, from wide-angle seismic data modelling converted to two-way travel-time, corresponds to the base of a series of reflectors in the corresponding reflection seismic section from the New Caledonia basin (Figure 15).

7. Results and discussion

Both wide-angle seismic profiles (Figures 8 and 9) show large variations of the crustal thickness, from 23 km beneath the Lord Howe Rise and the Fairway Ridge to 8 km in the basins. The crustal thickness underneath the Norfolk Rise on Profile S is around 17 km. The Moho depth of 26.5 km beneath Lord Howe Rise corresponds well with the 29 km maximum depth found from expanded spread seismic profiling [*Shor et al.*, 1971]. All three rises are covered by sedimentary sequences ranging from several hundred of meters up to 3 km in thickness. The deep crustal structure of all three rises is similarly characterised by 3 seismic layers. The first layer underneath the acoustic basement shows variable velocities between 4 and 5.8 km/s, and may correspond to either volcanic or sedimentary rocks. The second and third layers are characterized by velocities of 6.4 to 6.6 and 6.6 to 6.8 km/s. The interface between these layers is modelled as a second order velocity boundary, as no reflections are observed along this interface but simply a change in velocity gradient. A comparison of the velocity-depth profiles from the Lord Howe Rise and Fairway Ridge reveals a close resemblance to other continental fragments such as Lousy Bank and the Seychelles Plateau (For compilation see Carlson et al. [1980] and references therein) (Figure 16 (A)). Oceanic plateaus generally show steeper velocity gradients and a smaller crustal thickness than continental fragments. Volcanic islands are characterised by even steeper gradients and smaller crustal thickness. For the Lord Howe Rise a continental origin found in this study is in good agreement with results from expanding spread profiles [*Shor et al.*, 1971] and magnetic modelling [*Schreckenberger* *et al.*, 1992]. On the basis of the velocity gradients and crustal thicknesses obtained from our dataset it can be deduced that the Fairway Ridge and Norfolk Ridge are of continental origin like the Lord Howe Rise. The correlation between positive magnetic anomalies and basement highs in this region, which is found on both profiles (Figures 8 and 9) could be explained by continental crust with a considerable magnetization in the lower crust [*Schreckenberger et al.*, 1992].

In the basins of Profile N the sedimentary layer thickness increases to up to 5 km in the eastern part of the asymmetric New Caledonia Basin and 4 km in the more symmetric Fairway Basin. Sedimentary thickness is lower on Profile S, with up to 3 km in both basins. The crustal thickness decreases on Profile N to 8 km in New Caledonia Basin and to 10 km in the Fairway Basin. The Fairway Basin crust on Profile N is thicker than normal oceanic crust. The seismic velocities and the relative thickness of the crustal layers are identical to the Lord Howe Rise and Fairway Ridge. This indicates that the Fairway Basin results from thinning of continental crust during extension. On Profile S the crustal thickness of the Fairway Basin is around 12 to 15 km and the lower crust exhibits elevated lower crustal velocities as compared to the bordering Lord Howe Rise and Fairway Ridge. As in the north the crustal and the relative layer thicknesses correspond to thinned continental rather than oceanic crust. A possible explanation for the elevated lower crustal velocities and densities could be intrusions into the lower crust emplaced during the rifting of the basin.

Comparison of crustal velocity-depth profiles from the New Caledonia Basin on Profile N and Profile S to typical oceanic crust [*White et al.*, 1992] indicates that, although crustal thickness on both profiles is only slightly thicker than for oceanic crust, the seismic velocities found on the northern profile are not representative of oceanic crustal velocities (Figure 16 (B)). The upper crustal layer exhibits velocities higher than those usually found in normal oceanic crust. No typical magnetic oceanic anomalies are found in the basin (Figure 8 (C)).

In the Parece Vela back-arc basin in the northeast Pacific Ocean it has been shown from sampling that even intermediate to fast spreading oceanic crust can contain high percentages of upper mantle material of residual but still fertile composition, which otherwise is found on segment ends of medium fast spreading mid-ocean ridges or on very slow spreading ridges [*Ohara*, 2006; *Ohara et al.*, 2002]. This fact might be explained by lower mantle temperatures in the back-arc basins due to the presence of the cold subducting slab [*Abers et al.*, 2006]. Seismic velocities of serpentinised peridotites depend on their degree of serpentinisation, but are generally higher than those found typically in lower crustal layers (6.00-7.00 km/s) and lower than normal mantle velocities (8.00-8.40 km/s).

We therefore propose that the crust in the New Caledonia Basin on Profile N could consist to a high degree of serpentinised upper mantle peridotites generated during an amagmatic phase of seafloor spreading similar to crustal accretion at ultra-slow spreading centres [*Coakley and Cochran*, 1998; *Michael et al.*, 2003; *Jokat and Schmidt-Aursch*, 2006]. This hypothesis is additionally strengthened by the absence of oceanic magnetic anomalies, which are mainly produced by the basaltic layer of magmatically formed oceanic crust and crustal densities higher than those found in either normal oceanic or continental crust. The weak amplitude Moho reflection in the basin might then originate from the serpentinisation front, as has been proposed in very slow spreading ridge environements [*Jokat and Schmidt-Aursch*, 2006].

On Profile S the velocity-depth profile from the New Caledonia Basin is indicative of normal oceanic crust. The slightly elevated crustal densities in the New Caledonia Basin can by explained by the presence of oceanic crust. Also, the basement character in the basin changes from the northern Profile N, where it is characterised by large blocks, to the southern profile where it shows a roughness characteristic for oceanic crust, with highs 15-20 km spaced about apart (Figure 17 (a) and (b)). In the middle of the basin a pronounced basement high correlates with a 200 nT magnetic signature, which might correspond to an extinct spreading centre (Figure 17 (b)). The modelling of the magnetic anomalies in New Caledonian Basin indicates a crust of basaltic origin which is clearly correlated with the topography of the basin and the absence of magnetic anomalies [*Collot*, 2005]. The absence of magnetic anomalies in the basin can be explained by the fact that the basin is too narrow to span several magnetic reversals or that the crust was constructed during the Cretaceous quiet time [*Collot*, 2005].

Neighbouring segments along the spreading axis in back-arc basins can display highly contrasted axial morphologies as found in the North Fiji Basin [*Garel et al.*, 2003]. Bathymetric studies of the Fiji back-arc basin demonstrate that both axial highs typical of fast spreading, and valleys typical of slow and very slow spreading, can be found along a single segment. This fact can be explained by spatial variations in the distribution of upper mantle convection cells below accretion centers superimposed on the thermal anomaly located under the whole basin [*Garel et al.*, 2003]. We propose that theNew Caledonia Basin crust on Profile S is generated by a magmatically spreading segment, and therefore shows features typical for normal oceanic crust: a division into one two seismically distinguishable layers (the basaltic and the gabbroic layer), a basement roughness typical for oceanic crust, and an axial high corresponding to the spreading center. The much stronger Moho reflection (Figure 15) here originates from the base of the gabbroic layer.

Modelling of the wide-angle seimic data resulted in imaging for the first time a strong reflector in the upper mantle of the New Caledonia Basin (Figure 8). Documentation of mantle structures can help improve our understanding of how the subcrustal lithosphere is deformed and the relative behaviour between the crust and the upper mantle. The most widely studied mantle reflector is the Flannan reflector beneath the Devonian-Triassic West Orkney Basin off Scotland [*McBride et al.*, 1995], which has been imaged to a depth of about 80 km. Among the proposed mechanisms for the origin of this reflector are the Caledonian orogeny [*Brewer and Smythe*, 1984] as well as the subsequent basin extension [*Reston*, 1993; *Stein and Blundell*, 1990]. A later study proposed either differential extension of crust at least partially coupled to the uppermost mantle, or a broad zone of simple shear that was largely confined to the upper mantle but reactivated to deform the crust, as the origin for the Flannan mantle reflector [*McBride et al.*, 1995].

The top of one of the two low velocity zones underneath New Caledonia proposed from modelling of the source-receiver functions [*Regnier*, 1988] may correspond to the mantle reflector found in this study. In this case, the mantle reflector would represent to the top of a subducted plate from an earlier eastward subduction underneath New Caledonia. However, the westward deepening of the reflector does not fit to a proposed eastward dip of the low velocity zone. A strong mantle reflector at about 35 km depth has also been imaged beneath a 40 km-wide, back-arc extension zone on North Island, New Zealand, a geologic setting which may be similar to that of the New Caledonia Basin. The authors propose the origin of this reflector to be the top of a reservoir of partial melt [*Stratford* *and Stern*, 2004]. As no excessive volcanism has been found in the New Caledonia Basin this hypothesis seems unlikely for the New Caledonia Basin.

Although the landstation data do not allow to trace the mantle reflector in the vicinity of New Caledonia it general inclination suggests, that it gets in contact with the Moho underneath New Caledonia. Therefore, the most likely explanation of the origin of the mantle reflector is that it formed during the extensional phase of the New Caledonian basin and represents a shear zone in the mantle. No deep reflection has been modelled on Profile S, which might either be caused by the data quality or by the fact, that the reflector is confined to the middle segment of the New Caledonian Basin.

8. Conclusions

Modelling of the wide-angle seismic data from the ZONECO 11 cruise confirmed of the continental nature of the Lord Howe Ridge, and enabled the determination of nature of the crust of the Fairway Ridge and the Norfolk Rise, which are also shown to be continental. This strengthens the hypothesis that all three ridges formed by fragmentation of Gondwanaland, caused either by widespread extension or in a backarc setting.

The Fairway Basin shows relative layer thicknesses and upper crustal velocity gradients typical for thinned continental crust. Its lower crustal velocities indicate a continental origin on Profile N. Velocities are slightly elevated on the southern profile, which can be explained by intrusions into the lower crust. This would also explain the slightly higher density found from gravity modelling.

The crust in the New Caledonia Basin on Profile N was modelled using velocities which are higher than either typical oceanic or continental crust. We propose that the crust in this region consists to a high degree of serpentinised upper mantle material generated during an amagmatic phase of opening of the basin, as has been found on ultra-slow spreading centres. This implies the absence of oceanic magnetic anomalies and of an axial high, which would be consistent with magmatic spreading. On Profile S the basin shows typical oceanic seismic velocities and relative layer thicknesses. Its basement is also characterised by typical oceanic roughness. We therefore propose that extension in this area resulted in magmatic sea-floor spreading.

A mantle reflector dipping towards the west has been identified beneath the New Caledonian Basin. Its dip does not correspond to the top of a low velocity zone found underneath New Caledonia from receiver function analysis, which has been associated to an eastward subduction underneath the island [*Regnier*, 1988]. The absence of large amounts of volcanism seems to exclude its origin as the head of a melt-bearing zone as proposed for a similar reflector on the North island of New Zealand [*Stratford and Stern*, 2004]. One explanation could be that it probably originates from the extensional tectonics during opening of the New Caledonian Basin.

Acknowledgments.

We would like to thank the captain and the crew of the N/O Atalante. Acquisition and processing of the data was funded by the ZoNéCo program of the ADECAL (Agence de Développement Economique de la Nouvelle Calédonie) in cooperation with Ifremer (Institute Français de Recherche pour l'Exploitation de la mer) and the IFP (Institut Français du Pétrole). The GMT [*Wessel and Smith*, 1995] and Seismic Unix software package [*Stockwell*, 1999] were used in the preparation of this paper. We would like to thank B. Pontoise (IRD) for deploying the landstations and A. Nercessian and S. Rouzo for help in the data acquisition. We thank M.-A. Gutscher for help with the English. Many thanks also to B. Pelletier and N. F. Exon for reviews which helped improve the manuscript.

References

Abers, G. A., P. E. van Keken, E. A. Kneller, A. Ferris, and J. C. Stachnik, The thermal structure of subduction zones constrained by seismic imaging: Implications for slab dehydration and wedge flow, *Earth Planet. Sci. Lett., 241*, pp. 387–397, 2006.

Aitchison, J., G. Clarke, S. Meffre, and D. Cluzel, Eocene arc-continent collision in New Caledonia and implications for regional southwest Pacific tectonic evolution., *Geology, 23, 2*, pp. 161–164, 1995.

Auzende, J. M., S. van den Beuque, M. Regnier, Y. Lafoy, and P. A. Symonds, Origin of New Caledonian Ophiolite based on a French-Australian Transit (faust), *Mar. Geol., 162(2-4)*, pp. 225–236, 2000.

Avedik, F., V. Renard, J. Allenou, and B. Morvan, "Single bubble" air-gun array for deep exploration, *Geophysics, 58*, pp. 366–382, 1993.

Avias, J., Overthrust structure of the main ultrabasic New Caledonian massifs, *Tectonophysics 4(4-6)*, pp. 531–541, 1967.

Brewer, J. A., and D. K. Smythe, MOIST and the continuity of crustal reflector geometry along the Caledonian-Appalachian orogen, *J. Geol. Soc. London, 141*, pp. 105–120, 1984.

Burns, R. E., J. E. Andrews, and the scientific party, Site 208, Initial Reports of the Deep Sea Drilling Project, pp. 271–331, 1973.

Caress, D., M. McNutt, R. Detrick, and J. Mutter, Seismic imaging of hotspot-related crustal underplating beneath the Marquesas Islands, *Nature 373*, pp. 600–603, 1995.

Carlson, R. L., N. I. Christensen, and R. P. Moore, Anomalous crustal structures in ocean basins: Continental fragments and oceanic plateaus, *Earth Planet. Sci. Lett., 51*, pp. 171–180, 1980.

Charvis, P., M. A. Laesanpura, J. Gallart, A. Hirn, J.-C. Lépine, B. de Voogd, T. Minshull, Y. Hello, and B. Pontoise, Spatial distribution of hotspot material added into the lithosphere under la réunion, *J. Geophys. Res. 104*, pp. 2875–2893, 1999.

Christensen, N. I., and W. D. Mooney, Seismic velocity structure and composition of the continental crust; a global view, *J. Geophys. Res., 100, 6*, pp. 9761–9788, 1995.

Cluzel, D., J. C. Aitchison, and C. Picard, Tectonic accretion and underplating of mafic terranes in the Late Eocene intraoceanic fore-arc of New Caledonia (Southwest Pacific)): geodynamic implications, *Tectonophysics, 340*, pp. 23–59, 2001.

Coakley, B. J., and J. R. Cochran, Gravity evidence of very thin crust at the Gakkel Ridge (Arctic Ocean), *Earth Planet. Sci. Lett., 163*, pp. 81–95, 1998.

Cohen, J. K., and J. W. Stockwell, Seismic Unix Release 37: a free package for seismic research and processing, *Center for Wave Phenomena, Colorado School of Mines.*, 2003.

Collot, J., Amorce de synthèse des connaissances des bassins du sud ouest pacifique et hypothèses sur l'origine et la nature du bassin de nouvelle calédonie dans sa partie centrale : apport des données de la campagne zoneco-11., *Masters Thesis*, p. 61, 2005.

Collot, J.-Y., A. Malahoff, J. Recy, G. Latham, and F. Missegue, Overthrust emplacement of the New Caledonia Ophiolite: Geophysical evidence, *Tectonics, 6, 3*, pp. 215–232, 1987.

Crawford, A. J., S. Meffre, and P. A. Symonds, 120 to 0 ma tectonic evolution of the southwest pacific and analogous geological evolution of the 600 to 220 ma tasman fold belt system., *Geol. Soc. Australia Spc. Publ., 22*, pp. 377–397, 2003.

de Beuque, S. V., Evolution geologique du domaine peri-caledonien (Sud Ouest Pacifique), *Ph. D. Thesis, University of Brest*, p. 270pp, 1999.

de Beuque, S. V., J.-M. Auzende, Y. Lafoy, and F. Missegue, Tectonique et volcanisme tertiare sur a ride de lord howe (Sud-Ouest Pacifique, *C. R. Acad. Sci. Paris*, pp. 663–669, 1998.

Den, N., W. J. Ludwig, S. Murauchi, J. I. Ewing, H. Hotta, N. T. Edgar, T. Yoshii, T. Asanuma, K. Hagiwara, T. Sato, and S. Ando, Seismic-refraction measurements in the northwest Pacific basin, *J. Geophys. Res., 75*, p. 1421, 1969.

Dubois, J., J. Launay, and J. Recy, Uplift movements in New Caledonia-Loyalty Islands area and their plate tectonics interpretation, *Tectonophysics, 24*, pp. 133–150, 1974.

Eade, J. V., The Norfolk Ridge system and its margins, *In: The ocean basins and margins, Plenum. New York, United States*, pp. 303–324, 1988.

Etheridge, M. A., P. A. Symonds, and G. S. Lister, Application of the detachment model to reconstruction of conjugate passive margins, *AAPG Bull 46*, p. 23?40, 1989.

Exon, N., P. Hill, Y. Lafoy, M. Fellows, K. Perry, P. Mitts, R. R. Howe, G. Chaproniere, G. Dickens, B. Ussler, and C. Paull, Geology of the Fairway and New Caledonia Basins in the Tasman Sea from: sediment, pore water, diapirs and bottom simulating reflectors (Franklin Cruise FR9/ 01 and Geoscience Australia Survey 232), *Geoscience Australia Record 2004/26*, pp. 291–300, 2004.

Exon, N. F., Y. Lafoy, P. J. Hill, G. R. Dickens, and I. Pecher, Geology and petroleum potential of the Fairway Basin in the Tasman sea, *Australian J. Earth Sci.*, pp. 629–645, 2007.

Francis, T. J. G., and R. W. Raitt, Seismic refraction measurements in the southern Indian Ocean, *J. Geophys. Res., 72*, p. 3015, 1967.

Francis, T. J. G., D. Davies, and M. N. Hill, Crustal structure between kenya and the seychelles, *Philos. Trans. R. Soc. London, Ser. A, 259*, p. 240, 1966.

Gaina, C., D. R. Muller, J. Y. Royer, J. Stock, J. Hardebeck, and P. Symonds, The tectonic history of the Tasman Sea: A puzzle with 13 pieces, *Earth Planet. Sci. Lett., 197, 3-4*, pp. 273–286, 1998.

Garel, E., Y. Lagabrielle, and B. Pelletier, Abrupt axial variations along slow to ultra-slow spreading centers of the northern north Fidji Basin (sw pacific): Evidence for short wave heterogeneities in a back-arc mantle, *Mar. Geophys. Res., 24*, pp. 245–263, 2003.

Hammer, P. T. C., L. M. Dorman, and J. A. Hildebrand, Jasper seamount structure: Seafloor seismic refraction tomography, *J. Geophys. Res. 99*, pp. 6731–6752, 1994.

Jokat, W., and M. Schmidt-Aursch, Geophysical characterisitics of the ultra-slow spreading Gakkel Ridge, Arctic Ocean, *submitted to: Geophys. J. Int.*, 2006.

Klingelhoefer, F., T. A. Minshull, D. K. Blackman, P. Harben, and V. Childers, Crustal structure of Ascension Island from wide angle seismic data: implications for the formation of volcanic islands, *Earth Planet. Sci. Lett., 190*, pp. 41–56, 2001.

Klingelhoefer, F., R. A. Edwards, R. W. Hobbs, and R. W. England, Crustal structure of the NE-Rockall Trough from wide-angle seismic data modelling, *J. Geophys. Res., 110*, p. B11105, 2005.

Kroenke, L. W., Cenozoic tectonic development of the Southwest Pacific, *Committee for co-ordination of joint prospecting for mineral resources in South Pacific offshore areas (CCOP/SOPAC) Tech. Bull., New Zealand*, p. 122pp, 1984.

Lafoy, Y., and Ship. Sci. Party, Rapport de mission de la campagne zonéco 11 de sismique lourde (multitraces, réfraction, haute résolution) à bord du N/O L'Atalante (8 sept.-5 oct. 2004), p. 147, 2004.

Lafoy, Y., B. Pelletier, J. M. Auzende, F. Missegue, and L. Molard, Tectonique compressive Cénozoique sur les rides de Fairway et de Lord Howe, entre Nouvelle Calédonie et Australie, *C. R. Acad. Sci. Paris, 319*, pp. 1063–1069, 1994.

Lafoy, Y., I. Brodien, R. Vially, and N. F. Exon, Structure of the basin and ridge system west of New Caledonia (Southwest Pacific): A synthesis, *Mar. Geophys. Res., 26*, pp. 37–50, 2005a.

Lafoy, Y., L. Géli, F. Klingelhoefer, R. Vially, B. Sichler, and H. Nouzé, Discovery of continental stretching and oceanic spreading in the Tasman Sea, *EOS, 10*, pp. 101–108, 2005b.

Ludwig, J. W., J. E. Nafe, and C. L. Drake, Seismic refraction, *The Sea, 4, 1*, pp. 53–84, 1970.

McBride, H. H., D. B. Snyder, M. P. Tate, R. W. England, and R. W. Hobbs, Upper mantle reflector structure and origin beneath the Scottish Caledonides, *Tectonics, 14 (5)*, pp. 1351–1367, 1995.

Michael, P. J., G. H. Langmuir, H. J. B. Dick, J. E. Snow, S. L. Goldstein, K. Lehnert, G. Kurras, W. Jokat, R. Muehe, and H. N. Edmonds, Magmatic and amagmatic seafloor generation at the ultraslow-spreading Gakkel ridge, Arctic Ocean, *Nature, 423*, pp. 956–

961, 2003.

Mignot, A., Sismo-stratigraphie de la terminaison nord de la ride de lord howe, evolution geodynamique du sud-ouest pacifique entre l'australie et la nouvelle- caledonie, *Ph. D. Thesis, Universite Pierre et Marie Curie*, p. 203pp, 1984.

Ohara, Y., Mantle process beneath Philippine Sea back-arc spreading ridges: A synthesis of peridotite petrology and tectonics, *Island Arc, 15*, pp. 119–129, 2006.

Ohara, Y., R. J. Stern, T. Ishii, H. Yurimoto, and T. Yamazaki, Peridotites from the Mariana Trough: first look at the mantle beneath an active back-arc basin, *Contrib. Mineral. Petrol., 143*, pp. 1–18, 2002.

Paris, J. P., Sur l'âge éocène supérieur de la mise en place de la nappe ophiolithique de Nouvelle Calédonie déduit d'observations nouvelles sur la série de Népoui, *C. R. Acad. Sci. Paris, série D*, pp. 1659–1661, 1979.

Pelletier, B., Geology of the New Caledonia region and its implications for the study of the New Caledonian biodiversity, *In: Compendium of marine species from New Caledonia, C. Payri and B. Richer de Forges (Eds), forum Biodiversite des Ecosystemes Coralliens, Doc. Sci. Tech. IRD*, pp. 17–30, 2006.

Ravenne, C., C. E. de Broin, J. Dupont, A. Lapouille, and J. Launay, New Caledonia basin-Fairway Ridge: structural and sedimentary study, *In: Editions TECHNIP, International Symposium on Geodynamics in the South-West Pacific Nouméa, 1976*, pp. 145–154, 1977.

Regnier, M., Lateral variation of upper mantle structure beneath New Caledonia determined from P-wave receiver function: evidence for a fossil subduction zone, *Geophys. J.*, pp. 561–577, 1988.

Reston, T. J., Evidence for extensional shear zones in the mantle, offshore Britain, and their implication for the extension of the continental lithosphere, *Tectonics*, pp. 492–506, 1993.

Rigolot, P., and B. Pelletier, Tectonique compressive récente le long de la marge Ouest de la Nouvelle-Caledonie : Résultats de la campagne ZOE 400 du N/O Vauban (mars 1987), *C. R. Acad. Sci. Paris, 307 (II)*, pp. 179–184, 1988.

Sandwell, D., and W. Smith, Marine gravity from satellite altimetry, *The Geological Data Center, Scripps Institution of Oceanography, La Jolla, CA92093 (digital file, version 7.2), (anonymous ftp to baltica.ucsd.edu)*, 1995.

Schreckenberger, B., H. A. Roeser, and P. A. Symonds, Marine magnetic anomalies over the Lord Howe Rise and the Tasman sea: Implications for the magnetization of the lower continental crust, *Tectonophysics, 212*, pp. 77–97, 1992.

Sdrolias, M., D. R. Mueller, and C. Gaina, Tectonic evolution of the southwest pacific using constraints from backarc basins, *In: Evolution and dynamics of the Australian Plate, R. R. Hills and D. R. Mueller (eds), Geol. Soc. of America Spec. Pap. 372*, pp. 343–359, 2003.

Shor, G. G., H. K. Kirk, and H. W. Menard, Crustal structure of the Melanesian area, *J. Geophys. Res.*, pp. 2562–2586, 1971.

Smith, W., and D. Sandwell, Global seafloor topography from satellite altimetry and ship depth soundings, *Science 277*, pp. 1956–1962, 1997.

Stein, A. M., and D. J. Blundell, Geological inheritance and crustal dynamics of the northwest Scottish continental shelf, *Tectonophys.*, pp. 455–467, 1990.

Stockwell, J. W., The cwp/su: Seismic un*x package, *Computers and Geosciences*, 1999.

Stratford, W. R., and T. A. Stern, Strong seismic reflections and melts in the mantle of a continental back-arc basin, *Geophys. Res. Lett., 31*, 2004.

Sutherland, R., Basement geology and tectonic development of the greater New Zealand region: an interpretation from regional magnetic data, *Tectonophys. 308*, pp. 341–362, 1999.

Sutton, G. H., G. L. Maynard, and D. M. Hussong, Widespread occurrence of a high-velocity basal layer in the Pacific crust found with repetitive sources and sonobuoys, *in: The structure and physical properties of the earth's crust, ed. J. G. Heacock, Am. Geophys. Union*, p. 193, 1971.

Symonds, P. A., J. B. Colwell, H. I. M. Struckmeyer, J. B. Willcox, and P. J. Hill, Mesozoic rift basin developement off eastern australia, *Geol. Soc. Aust. Abstr. 43*, pp. 528–542, 1996.

Uruski, C., and R. Wood, A new look at the new caledonia basin, an extension of the taranaki basin, offshore north island, new zealand, *Mar. Pet. Geol., 8*, pp. 379–391, 1991.

Vially, R., Y. Lafoy, J. M. Auzende, and R. France, Petroleum potential of New Caledonia and its offshore basins, *AAPG int. Conf., Barcelona, Spain*, pp. 1–6, 2003.

Watts, A., U. ten Brink, P. Buhl, and T. Brocher, A multichannel seismic study of lithospheric flexure across the hawaiian -emperor seamount chain, *Nature 315*, pp. 105–111, 1985.

Watts, A. B., C. Peirce, J. Colier, R. Dalwood, J. P. Canales, and T. J. Henstock, A seismic study of lithospheric flexure in the vicinity of Tenerife, Canary Islands, *Earth Planet. Sci. Lett. 146*, pp. 431–447, 1997.

Weissel, J. K., and D. E. Hayes, Evolution of the Tasman Sea reappraised, *Earth Planet. Sci. Lett., 25, 1-3*, pp. 231–277, 1977.

Wessel, P., and W. H. F. Smith, A new version of the Generic Mapping Tool (GMT), *EOS, Trans. Am. Geophys. Un., 76*, p. 329, 1995.

White, R. S., D. McKenzie, and R. O'Nions, Oceanic crustal thickness from seismic measurements and rare earth element inversions, *J. Geophys. Res. 97*, pp. 19,683–19,715, 1992.

Willcox, J. B., P. A. Symonds, K. Hinz, and D. Bennett, Lord Howe Rise, Tasman Sea, preliminary geophysical results and petroleum prospects, *BMR Journal of Australian Geology and Geophysics. 5; 3, 225-236*, pp. 225–236, 1980.

Willcox, J. B., J. Sayers, H. M. J. Stagg, and S. V. de Beuque, Geogical framework of the Lord Howe Rise and adjacent ocean basins, *In Hill K.C., Bernecker T. (Eds.) Eastern Australian Basins Symposium. A refocused energy perspective for the future, Exploration Soc. of Australia, Spec. Publ.*, pp. 211–225, 2001.

Woodward, D. J., and T. M. Hunt, Crustal structure across the Tasman Sea, *N. Z. J. Geol. Geophys. 14(1)*, pp. 39–45, 1971.

Zelt, C. A., Modelling strategies and model assessment for wide-angle seismic traveltime data, *Geophys. J. Int. 139*, pp. 183–204, 1999.

Zelt, C. A., and R. B. Smith, Seismic travel time inversion for 2-d crustal velocity structure, *Geophys. J. Int. 108*, pp. 16–31, 1992.

9. Figure Captions

Figure 1: (A) Predicted bathymetry from satellite altimetry [*Smith and Sandwell*, 1997] of the study region in the southwest Pacific. Bold line show wide-angle profiles and major

physiographic features are annotated. (B) Location map of the wide-angle seismic profiles (Box in A). Circles show OBS locations and inverted triangles IRD landstations. Contours are predicted seafloor bathymetry from satellite gravity [*Smith and Sandwell*, 1997] in an 1000m interval.

Figure 2: (a) Bandpass filtered (3-5 Hz, 24-36 Hz) vertical geophone data section from OBS 04 located in the New Caledonia Basin on Profile N. The data are displayed with a gain proportional to source-receiver offset and are reduced at a velocity of 6 km/s. PmP (reflection from the Moho), Pm2P (reflection from the deep mantle reflector) and Pn (turning waves fromt he upper mantle) are annotated (b) Synthetic seismograms calculated from the velocity model for the same station using the finite-difference modelling code from the Seismic Unix package [*Cohen and Stockwell*, 2003; *Stockwell*, 1999]. The synthetic seismograms are calculated every 100 m with a source frequency centred around 5 Hz. The deep mantle reflection is not reproduced because no velocity increase is associated to the reflector.

Figure 3: (a) Data from the vertical geophone data section from OBS 13 located on the Fairway Ridge on Profile N. The same gain, filter and scaling have been applied as in Figure 2 a. (b) Corresponding synthetic seismograms calculated from the model using the same method as in Figure 2 b.

Figure 4: (a) Data from the vertical geophone data section from OBS 16 located in the Fairway Basin on Profile N. The same gain, filter and scaling have been applied as in Figure 2 a. (b) Corresponding synthetic seismograms calculated from the model using the same method as in Figure 2 b.

Figure 5: (a) Data from the vertical geophone data section from OBS 35 located on the Norfolk Ridge on Profile S. The same gain, filter and scaling have been applied as in Figure 2 a. (b) Corresponding synthetic seismograms calculated from the model using the same method as in Figure 2 b.

Figure 6: (a) Data from the vertical geophone data section from OBS 42 located in the New Caledonia Basin on Profile S. The same gain, filter and scaling have been applied as in Figure 2 a. (b) Corresponding synthetic seismograms calculated from the model using the same method as in Figure 2 b.

Figure 7: (a) Data from the vertical geophone data section from OBS 53 located on the Lord Howe Rise on Profile S. The same gain, filter and scaling have been applied as in Figure 2 a. (b) Corresponding synthetic seismograms calculated from the model using the same method as in Figure 2 b.

Figure 8: (A) Final velocity model of Profile N including the model boundaries used during inversion (solid lines) and isovelocity contours every 0.25 km/s. Positions of OBSs (red circles) and landstations (orange inverted triangles) are indicated. Shaded areas are constrained by rays from the modelling. (B) shipboard measured magnetic anomaly along Profile N.

Figure 9: (A) Final velocity model of Profile S including the model boundaries used during inversion (solid lines) and isovelocity contours every 0.25 km/s. Positions of OBSs (red circles) are indicated. Shaded areas are constrained by rays from the modelling. (B) shipboard measured magnetic anomaly along Profile S.

Figure 10: (A) Ray coverage of the sedimentary layers of Profile N with every tenth ray from two-point ray-tracing plotted. Lower panel: Observed traveltime picks and

calculated travel times (line) of the sedimentary layers for all receivers along the Profile N. (B) Same as (A) but for the crustal layers (C) Same as (A) but for the Moho and upper mantle layers. (D) Same as (A) but for Profile S (E) Same as (D) but for crustal layers (E) Same as (D) but for the Moho and upper mantle layers.

Figure 11: (a) Resolution parameter for all depth nodes of the velocity model of Profile N. OBS positions are marked by black circles. Contour interval is 0.1. Depth uncertainty of the most important model boundaries as determined by 95% confidence limit of the F-test during depth perturbation of the boundary is given in the framed boxes. (b) Resolution parameter for all depth nodes of the velocity model of Profile S. OBS positions are marked by black circles. Contour interval is 0.1. The depth uncertainty of the most important boundaries calculated from the 95 % confidence limit of the f-test is given in the framed boxes.

Figure 12: Free air gravity anomaly in the study area from satellite altimetry [*Sandwell and Smith*, 1995], contoured every 10 mGal. The gravity anomaly north of Profile S causes a discrepancy between measured gravity by satellite and predicted gravity anomaly from modelling (marked by arrow).

Figure 13: (A) Upper panel: Shipboard measured free-air gravity anomaly (black line) and predicted anomaly from modelling (dashed line) along Profile N. Lower panel: Gravity model of Profile N. Positions of OBSs (circles) and landstations (inverted triangles) are indicated. Italic numbers give densities used for gravity modelling in g/cm^3. Black line indicate layer boundaries from seismic modelling and dashed lines additional boundaries for gravity modelling. (B) Upper panel: Shipboard measured free-air gravity anomaly (black line) and predicted anomaly from modelling (dashed line) along Profile S. Lower

panel: Gravity model of Profile S. Positions of OBSs (circles) are indicated. Italic numbers give densities used for gravity modelling in g/cm^3. Black line indicate layer boundaries from seismic modelling and dashed black lines addition boundaries for gravity modelling.

Figure 14: (A) Migrated multichannel seismic section of Profile N. OBS positions are indicated by black circles and layer boundaries from wide-angle data modelling by black lines. Blow-up of figure 17 is marked by squares. (B) Migrated multichannel seismic section of Profile S. OBS positions are indicated by black circles and layer boundaries from wide-angle data modelling by black lines. Blow-up of figures 17 and 15 is marked by square.

Figure 15: Migrated multichannel seismic section of reflections from the Moho in the New Caledonia Basin of Profile N. Predicted arrival time from wide-angle seismic modelling is indicated by the broken black line.

Figure 16: (A) Comparison of crustal velocity-depth profiles from the New Caledonia basin on Profile N (1) and Profile S (2) with typical oceanic crust (grey shade area gives envelope of velocities from the compilation of White et al., 1992). (B) Comparison of velocity depth profiles for different oceanic plateaus (broken black lines), continental fragments (black lines) and volcanic islands (dotted black lines): (1) Fiji Plateau [*Sutton et al.*, 1971] (2) Shatsky Rise [*Den et al.*, 1969] (3) Broken Ridge [*Francis and Raitt*, 1967], (4) Fairway Ridge (5) Lord Howe Rise (6) Lousy Bank [*Klingelhoefer et al.*, 2005] (7) Seychelles Plateau [*Francis et al.*, 1966] (8) Tenerife [*Watts et al.*, 1997] (9) Réunion [*Charvis et al.*, 1999] (10) Jasper Seamount [*Hammer et al.*, 1994] (11) Marquesas [*Caress et al.*, 1995] (12) Hawaii [*Watts et al.*, 1985] (13) Ascension [*Klingelhoefer et al.*, 2001].

Figure 17: Comparison of reflection seismic sections from the New Caledonia Basin along Profile N (A) and Profile S (B).

Figure 18: Blow-up reflection seismic section of the sedimentary layers in the New Caledonia Basin on Profile N and the parallel reflection seismic Profile Z11-02 about 25 km to the north (see Figure 1 for location).

Phase		No of picks	RMS traveltime residual	chi-squared
Water	1	4440	0.029	0.086
Sediments 1	2	19	0.025	0.068
Sediments 1 reflection	4	1029	0.079	0.619
Sediments 2	3	609	0.096	0.927
Sediments 2 reflection	5	899	0.088	0.782
Sediments 3	9	271	0.062	0.391
Basement reflection	17	224	0.146	2.136
Upper crust	14	7528	0.134	1.778
lower crust	11	4703	0.157	2.473
PmP	7	4342	0.182	3.293
Pn	8	346	0.149	2.227
Mantle reflection	13	355	0.772	59.695
All Phases		27005	0.159	2.529

Table 1. Traveltime residuals and chi-squared error for all phases and the complete model of Profile N.

Phase		No of picks	RMS traveltime residual	chi-squared
Water	1	3374	0.024	1.428
Sediments 1	2	94	0.076	2.629
Sediments 1 reflection	4	1187	0.051	3.534
Sediments 2	3	789	0.095	0.896
Basement reflection	17	250	0.121	9.808
Upper crust	14	8114	0.107	1.147
lower crust	11	2247	0.111	10.148
PmP	7	3283	0.130	13.476
Pn	8	1011	0.108	2.690
All Phases		22051	0.100	4.655

Table 2. Traveltime residuals and chi-squared error for all phases and the complete model of Profile S.

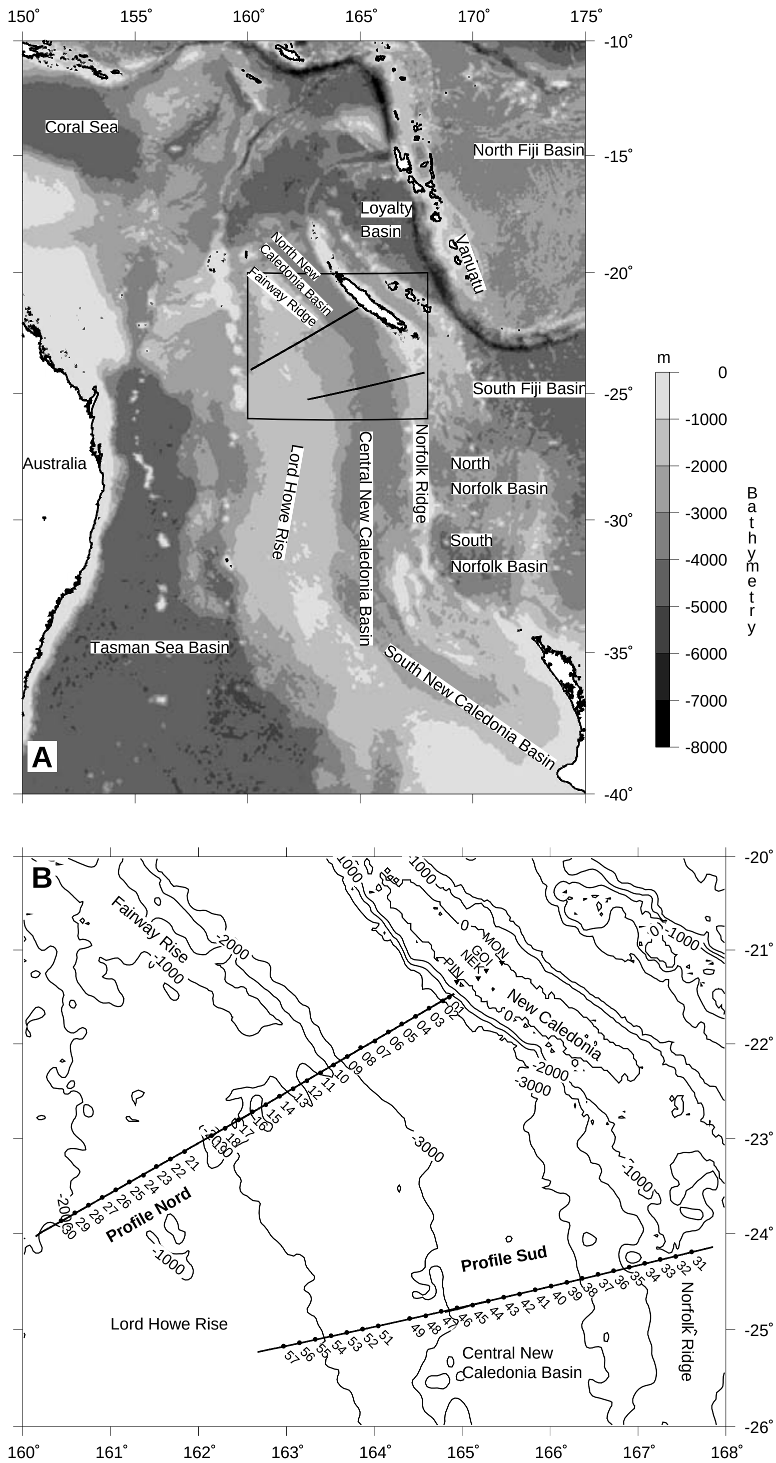

A
Coral Sea
North Fiji Basin
Loyalty Basin
Vanuatu
North New Caledonia Basin
Fairway Ridge
South Fiji Basin
Australia
Lord Howe Rise
Central New Caledonia Basin
Norfolk Ridge
North Norfolk Basin
South Norfolk Basin
Tasman Sea Basin
South New Caledonia Basin
Bathymetry
m
B
Fairway Rise
New Caledonia
Profile Nord
Profile Sud
Lord Howe Rise
Central New Caledonia Basin
Norfolk Ridge

Figure 1.

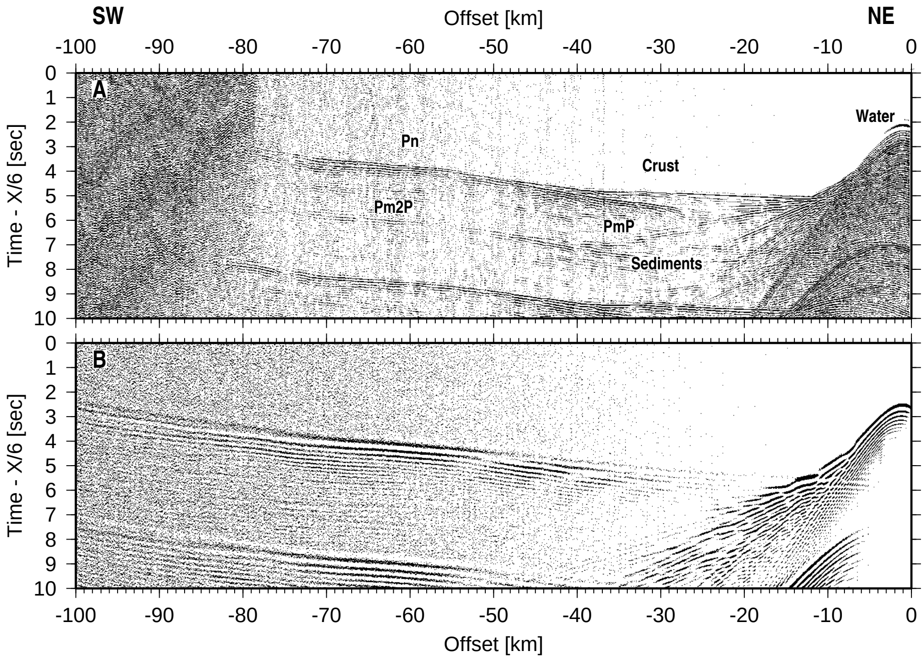
SW
Offset [km]
NE
A
Pn
Crust
Water
Pm2P
PmP
Sediments
Time - X/6 [sec]
B
Time - X/6 [sec]
Offset [km]

Figure 2.

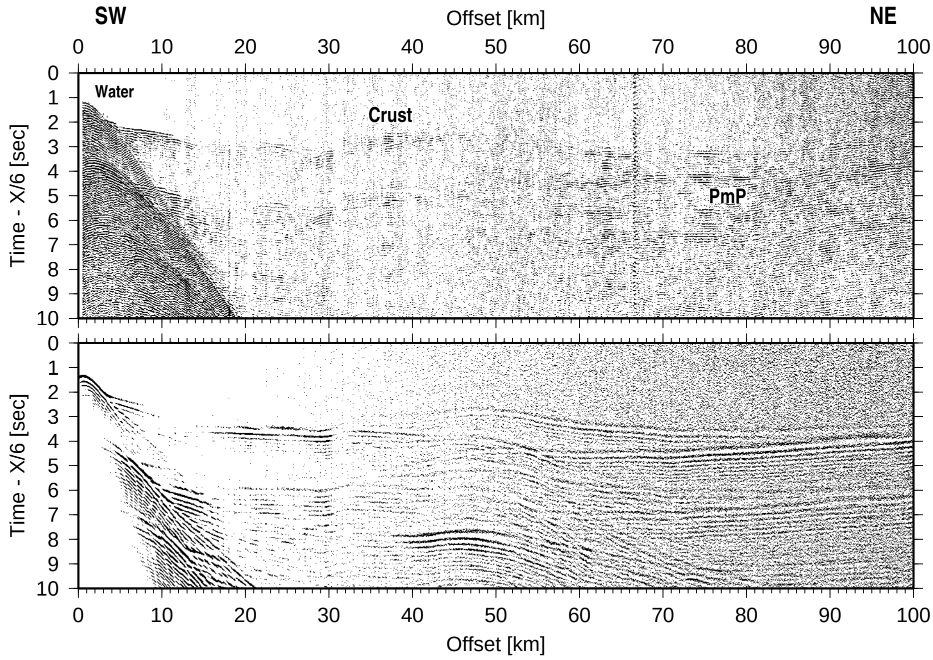
SW
Offset [km]
NE
Water
Crust
PmP
Time - X/6 [sec]
Time - X/6 [sec]
Offset [km]

Figure 3.

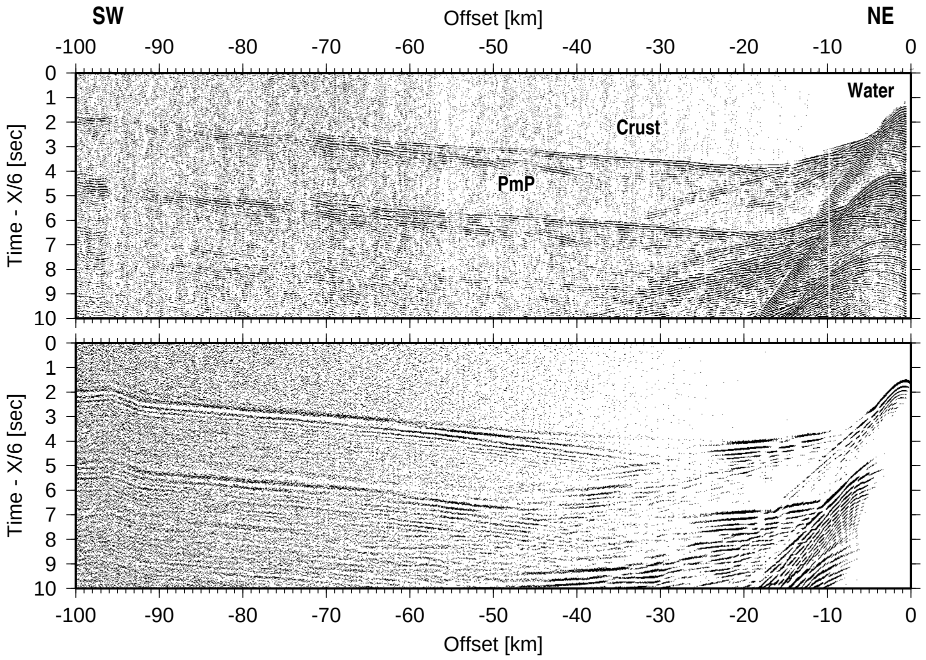
SW
NE
Offset [km]
Water
Crust
PmP
Time - X/6 [sec]
Time - X/6 [sec]
Offset [km]

Figure 4.

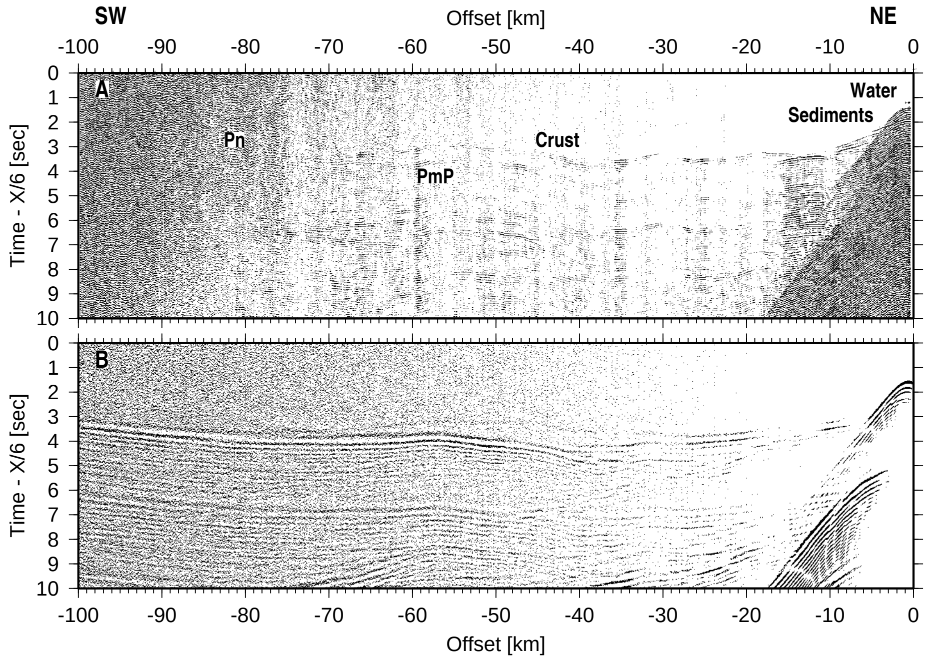
SW
Offset [km]
NE
-100
-90
-80
-70
-60
-50
-40
-30
-20
-10
0
A
Pn
PmP
Crust
Water
Sediments
Time - X/6 [sec]
B
Time - X/6 [sec]
Offset [km]

Figure 5.

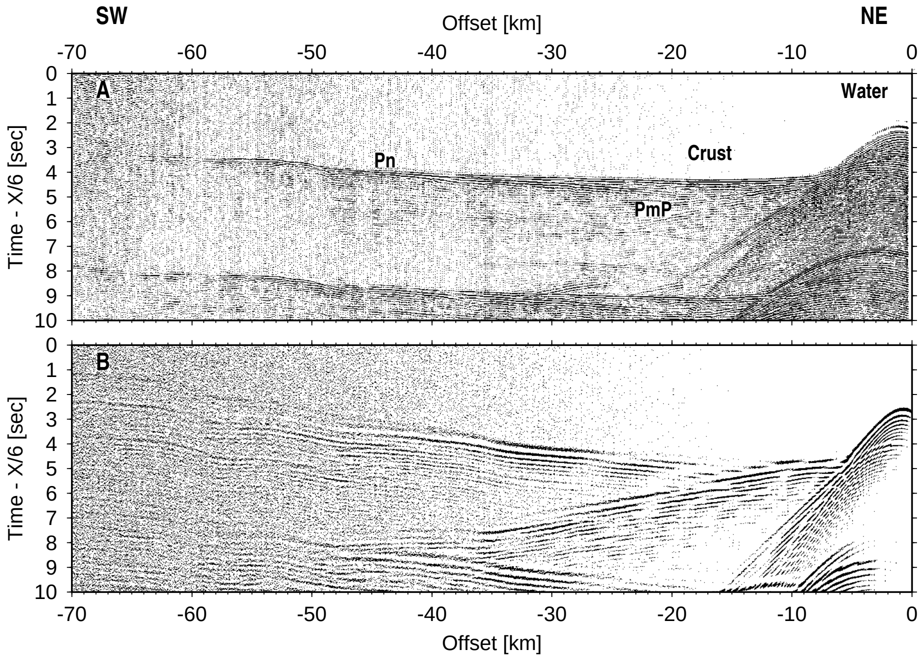
SW
NE
Offset [km]
-70
-60
-50
-40
-30
-20
-10
0
A
Water
Pn
Crust
PmP
Time - X/6 [sec]
B
Time - X/6 [sec]
Offset [km]

Figure 6.

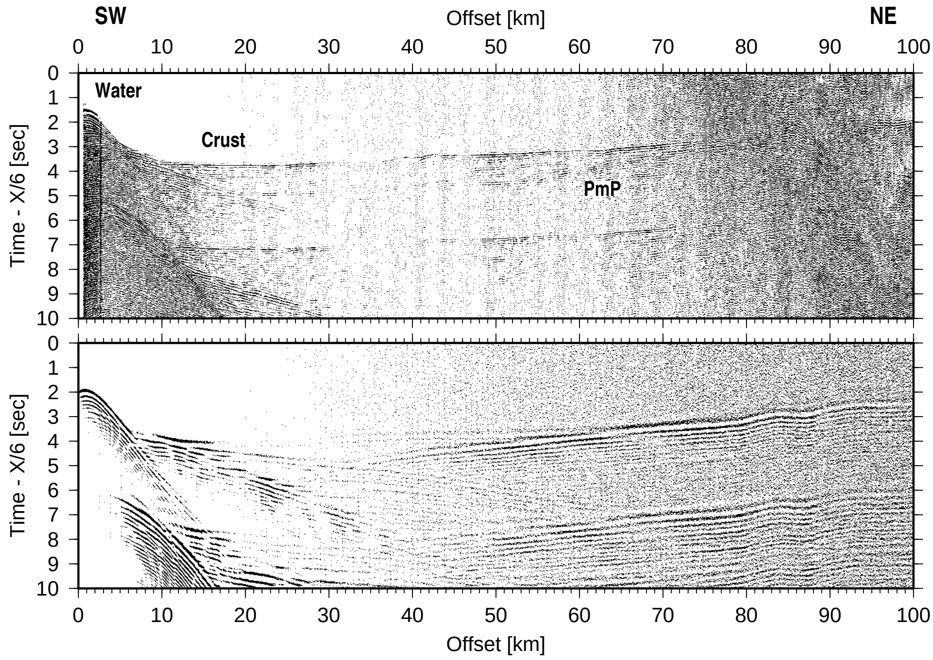
SW
Offset [km]
NE
Water
Crust
PmP
Time - X/6 [sec]
Time - X/6 [sec]
Offset [km]

Figure 7.

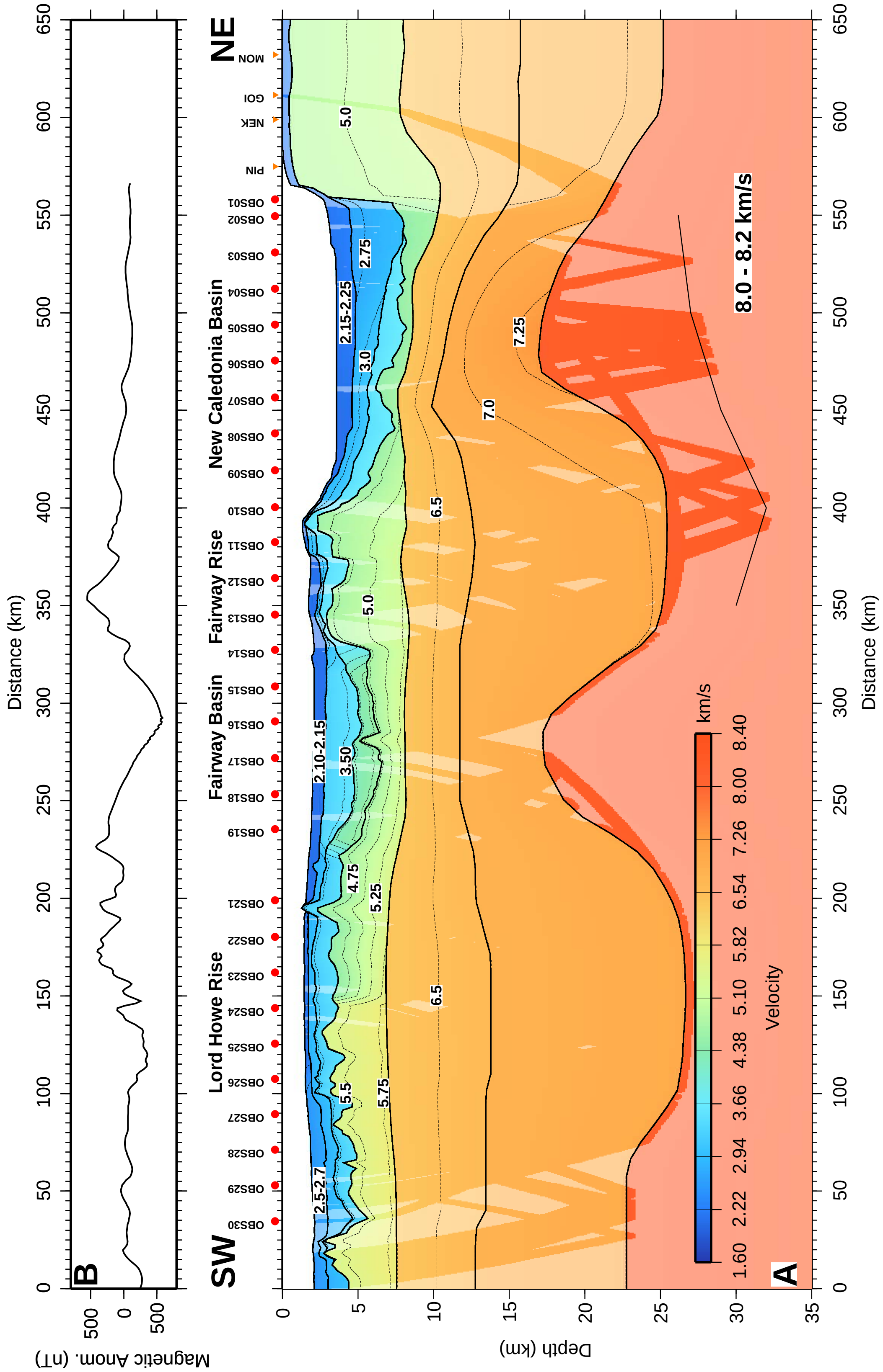
SW
NE
Lord Howe Rise
Fairway Basin
Fairway Rise
New Caledonia Basin
Distance (km)
Depth (km)
Magnetic Anom. (nT)
Velocity
km/s
8.0 - 8.2 km/s
A
B

Figure 8.

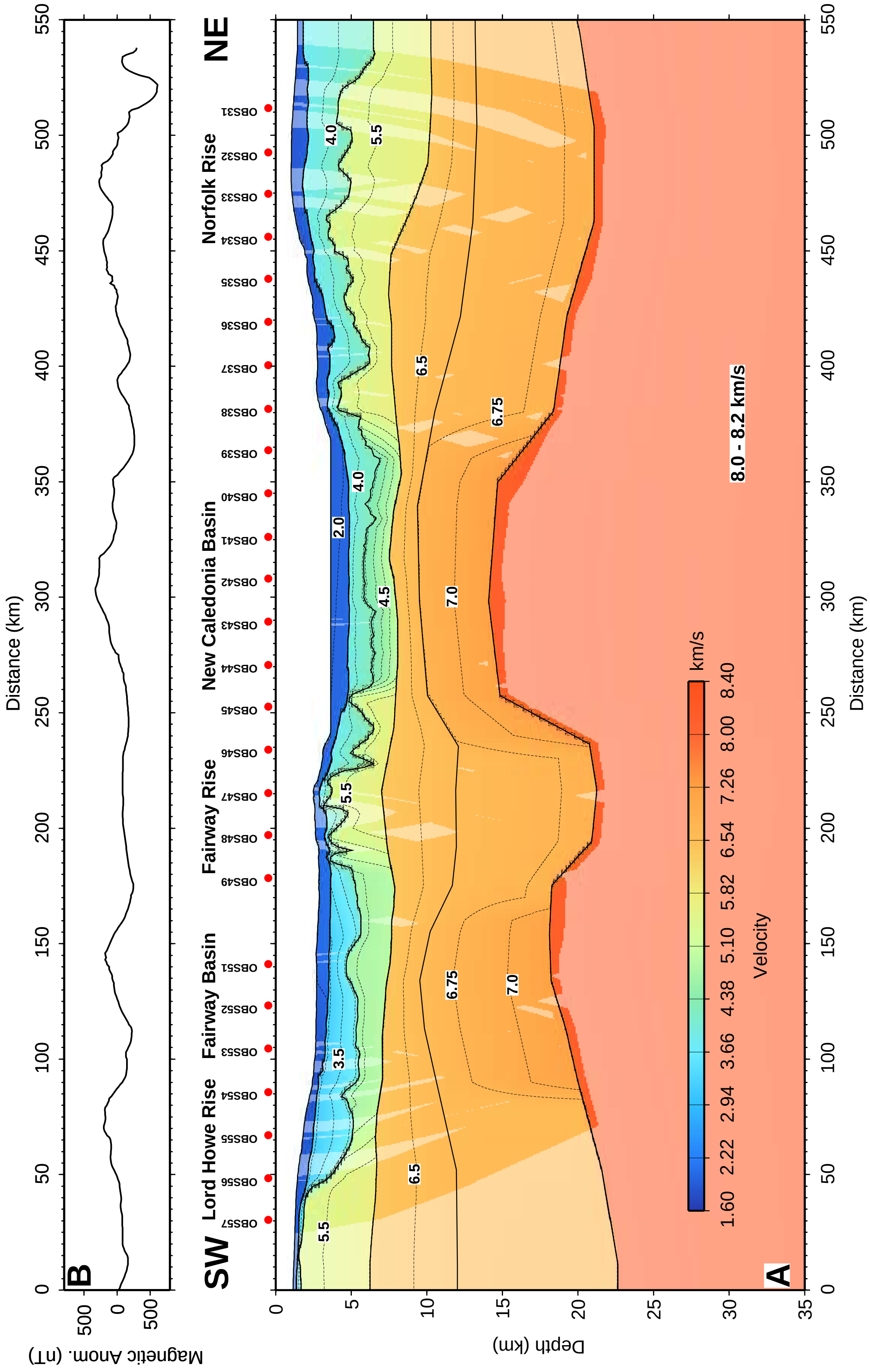
SW
NE
Lord Howe Rise
Fairway Basin
Fairway Rise
New Caledonia Basin
Norfolk Rise
OBS57
OBS56
OBS55
OBS54
OBS53
OBS52
OBS51
OBS49
OBS48
OBS47
OBS46
OBS45
OBS44
OBS43
OBS42
OBS41
OBS40
OBS39
OBS38
OBS37
OBS36
OBS35
OBS34
OBS33
OBS32
OBS31
A
B
Distance (km)
Depth (km)
Magnetic Anom. (nT)
8.0 - 8.2 km/s
Velocity
km/s
1.60 2.22 2.94 3.66 4.38 5.10 5.82 6.54 7.26 8.00 8.40

Figure 9.

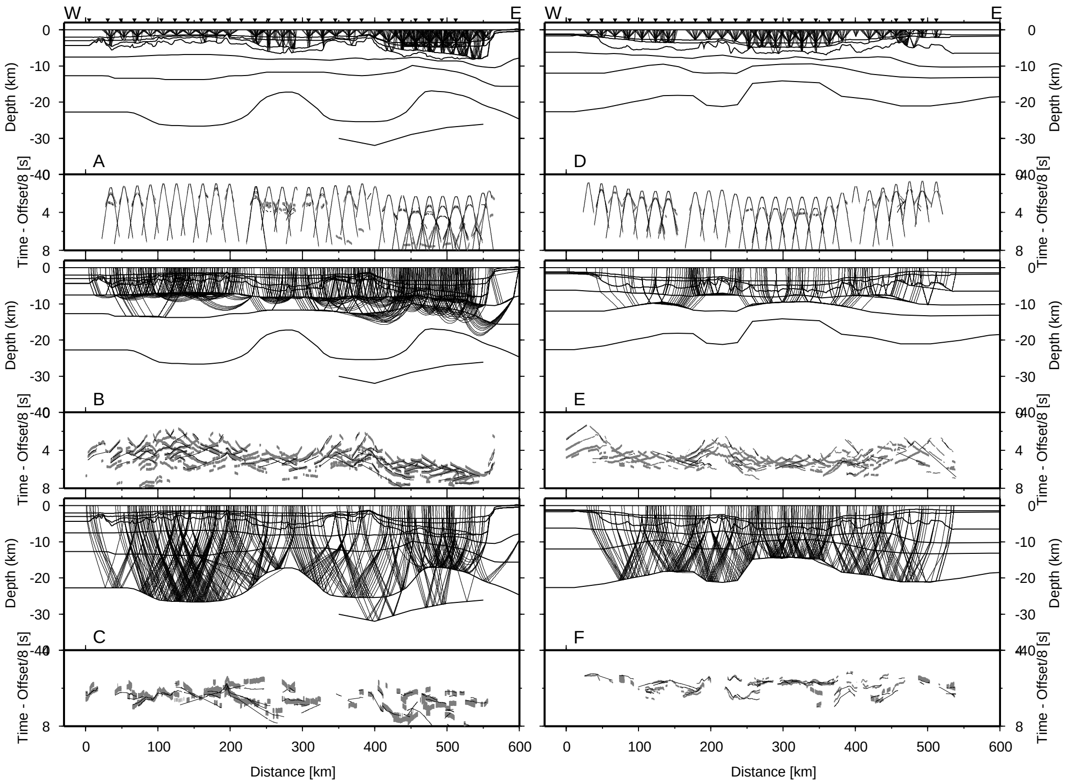
W
E
W
E
Depth (km)
Time - Offset/8 [s]
A
B
C
D
E
F
Distance [km]
0
-10
-20
-30
-40
4
8
0
100
200
300
400
500
600

Figure 10.

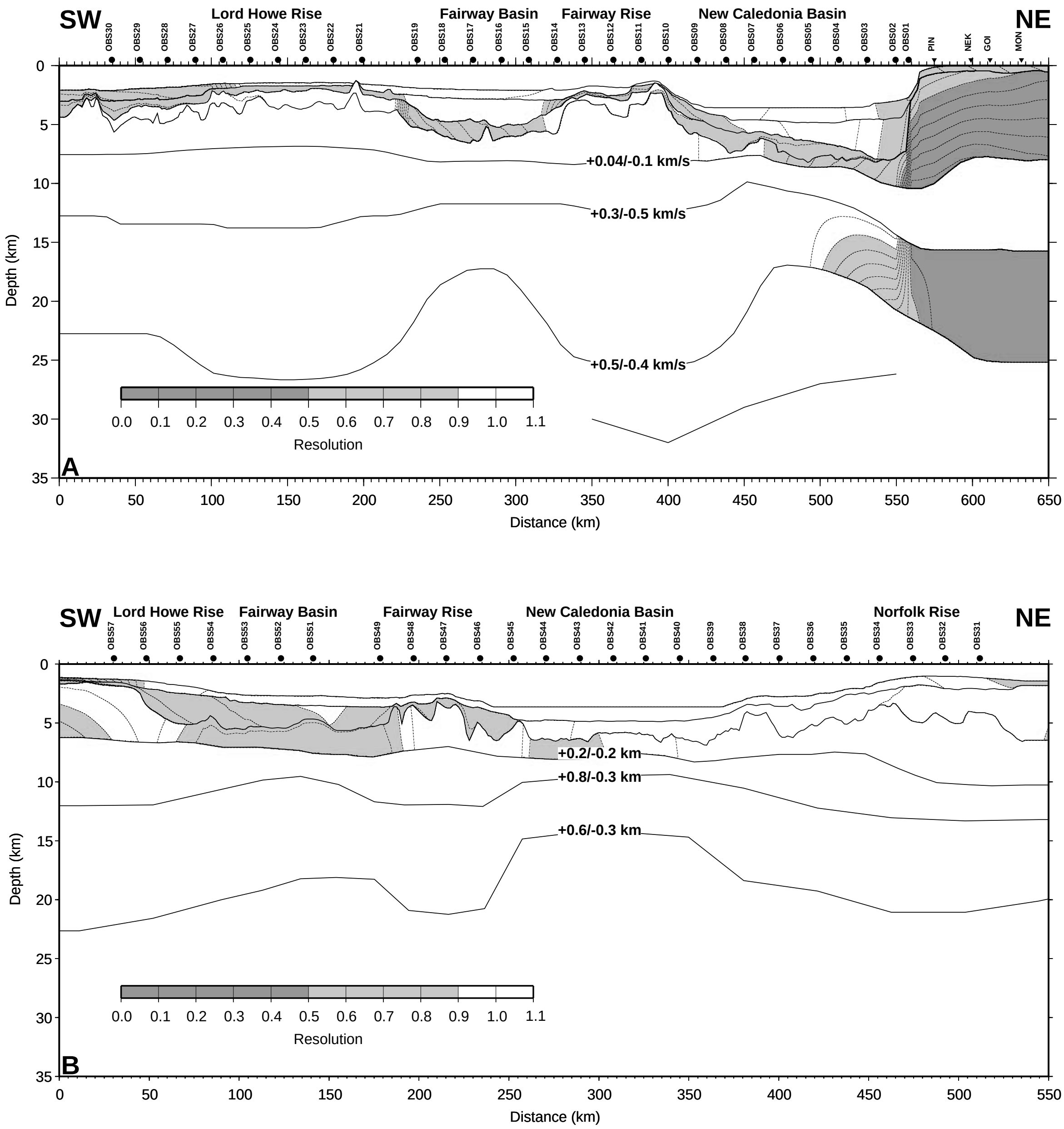
SW
Lord Howe Rise
Fairway Basin
Fairway Rise
New Caledonia Basin
NE
+0.04/-0.1 km/s
+0.3/-0.5 km/s
+0.5/-0.4 km/s
Resolution
Depth (km)
Distance (km)
A
Lord Howe Rise
Fairway Basin
Fairway Rise
New Caledonia Basin
Norfolk Rise
+0.2/-0.2 km
+0.8/-0.3 km
+0.6/-0.3 km
B

Figure 11.

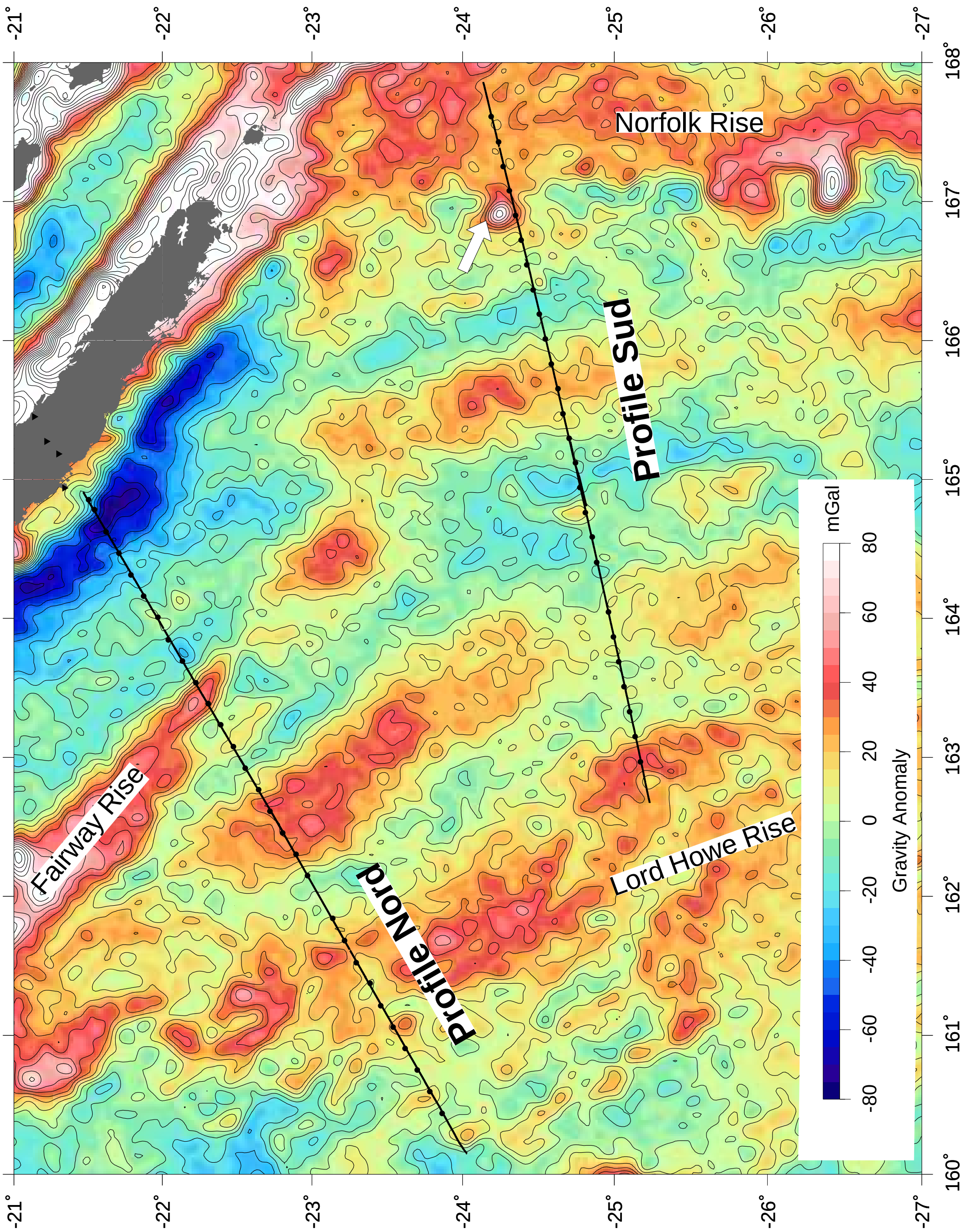
Norfolk Rise
Profile Sud
Profile Nord
Fairway Rise
Lord Howe Rise
mGal
Gravity Anomaly
80
60
40
20
0
-20
-40
-60
-80
-21˚
-22˚
-23˚
-24˚
-25˚
-26˚
-27˚
160˚
161˚
162˚
163˚
164˚
165˚
166˚
167˚
168˚

Figure 12.

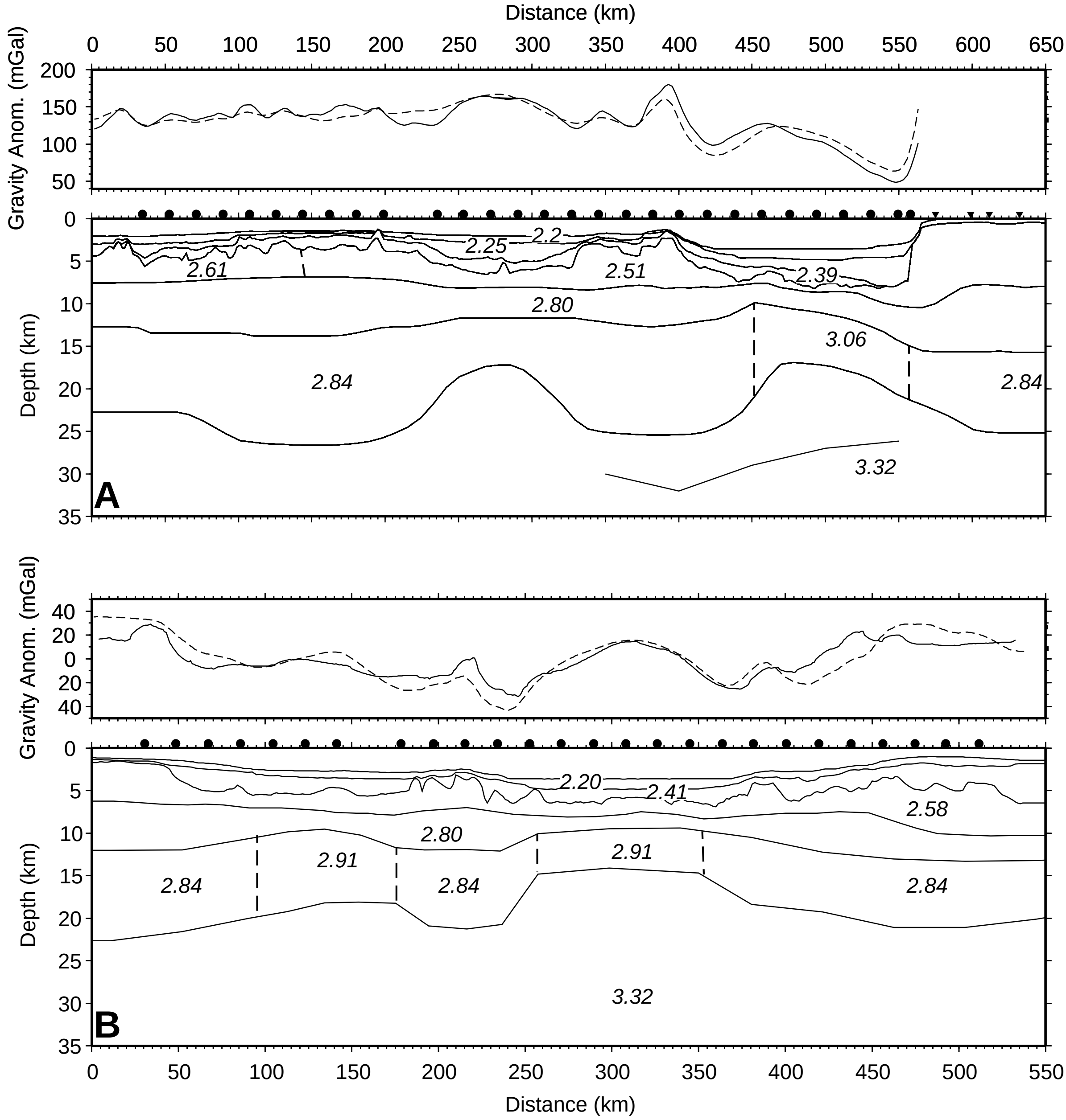
Distance (km)
Gravity Anom. (mGal)
Depth (km)
2.2
2.25
2.61
2.51
2.39
2.80
3.06
2.84
2.84
3.32
A
Gravity Anom. (mGal)
Depth (km)
2.20
2.41
2.58
2.80
2.91
2.91
2.84
2.84
2.84
3.32
B
Distance (km)

Figure 13.

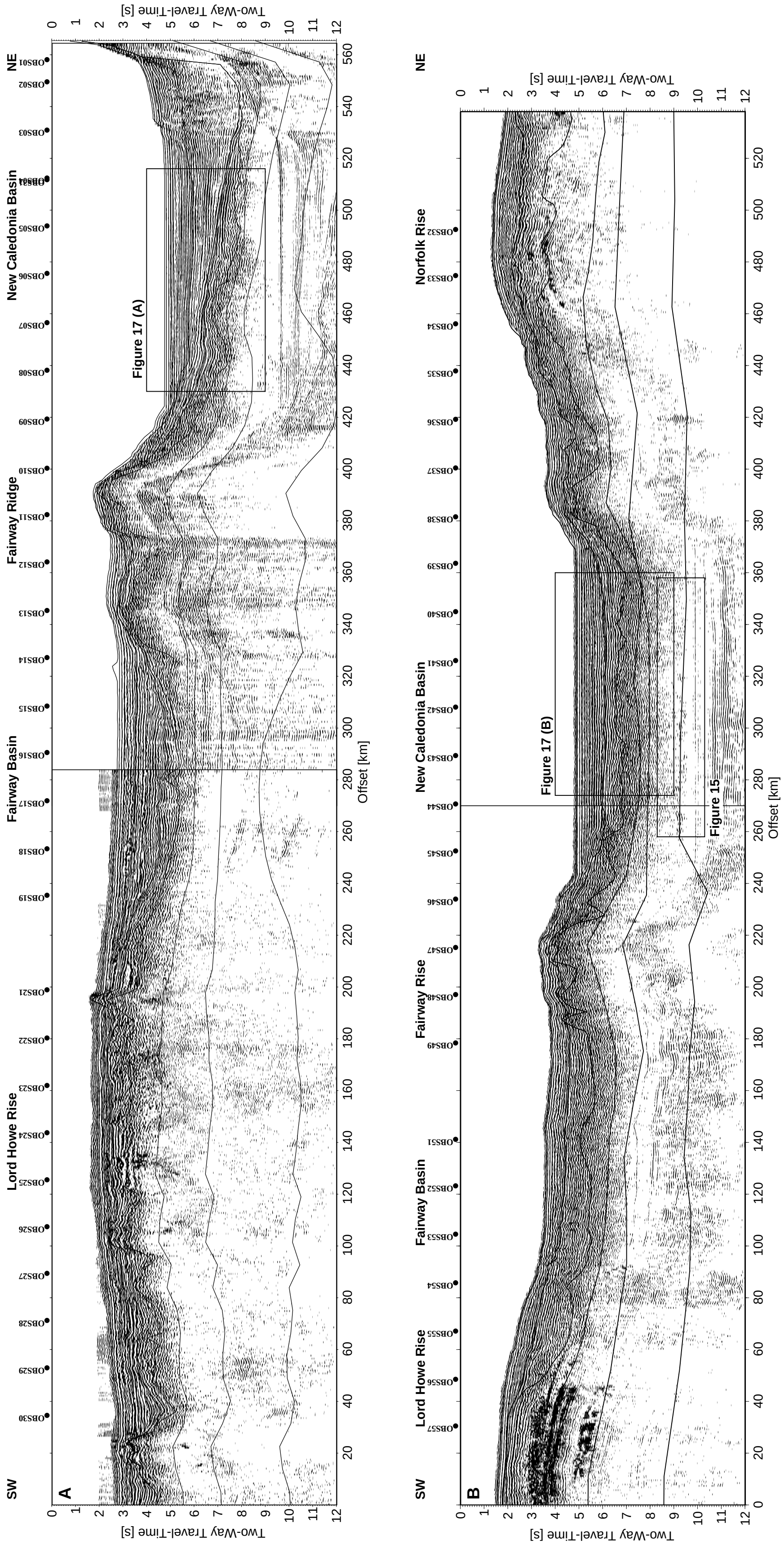
A
B
SW
NE
Lord Howe Rise
Fairway Basin
Fairway Ridge
Fairway Rise
New Caledonia Basin
Norfolk Rise
Figure 17 (A)
Figure 17 (B)
Figure 15
Offset [km]
Two-Way Travel-Time [s]

Figure 14.

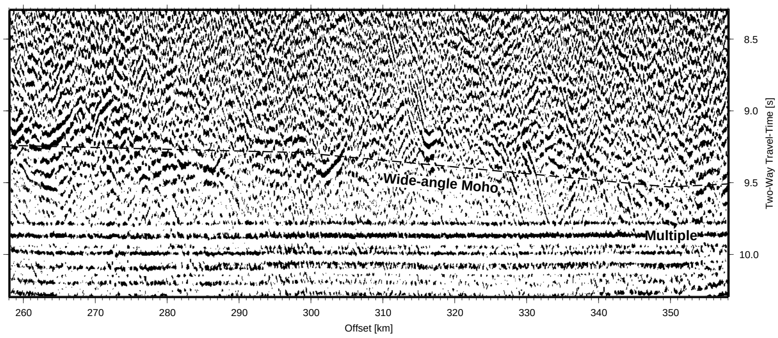
Wide-angle Moho
Multiple
8.5
9.0
9.5
10.0
Two-Way Travel-Time [s]
260
270
280
290
300
310
320
330
340
350
Offset [km]

Figure 15.

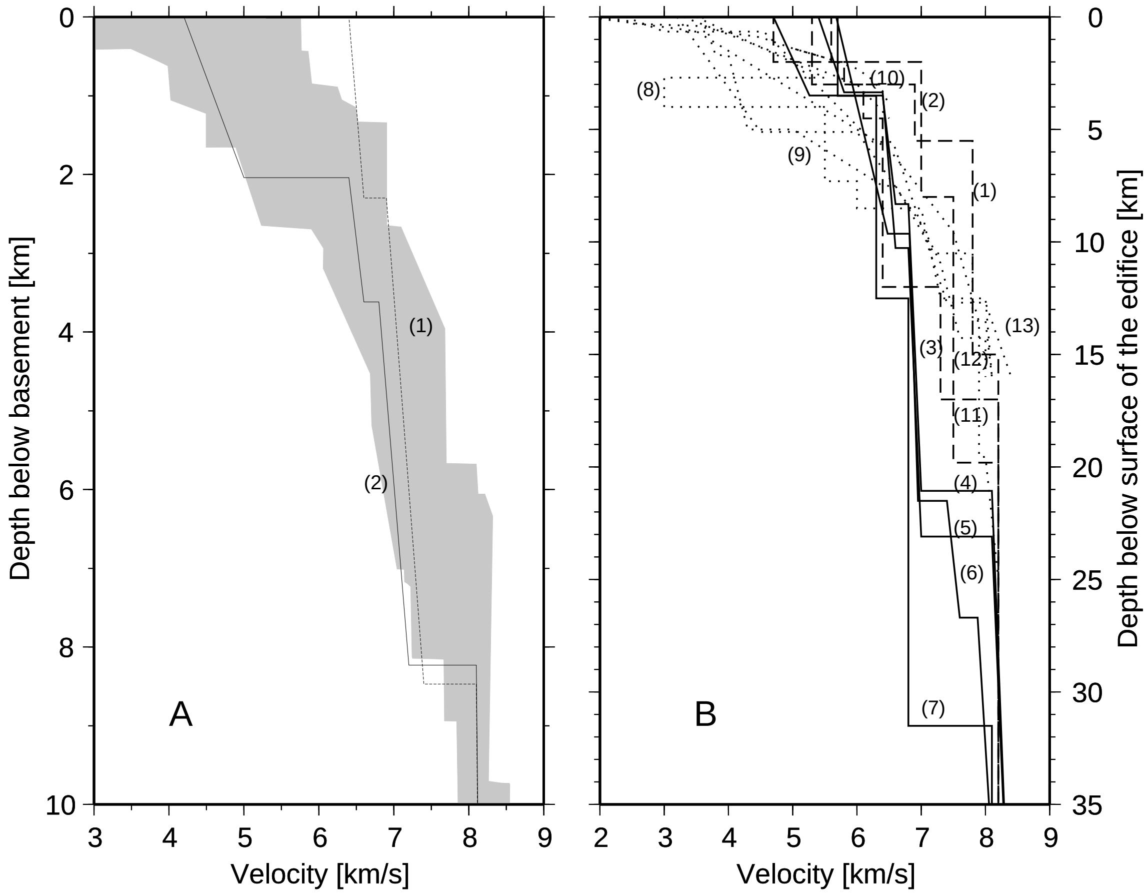

Depth below basement [km]
Velocity [km/s]
A
(1)
(2)
B
Depth below surface of the edifice [km]
(1)
(2)
(3)
(4)
(5)
(6)
(7)
(8)
(9)
(10)
(11)
(12)
(13)

Figure 16.

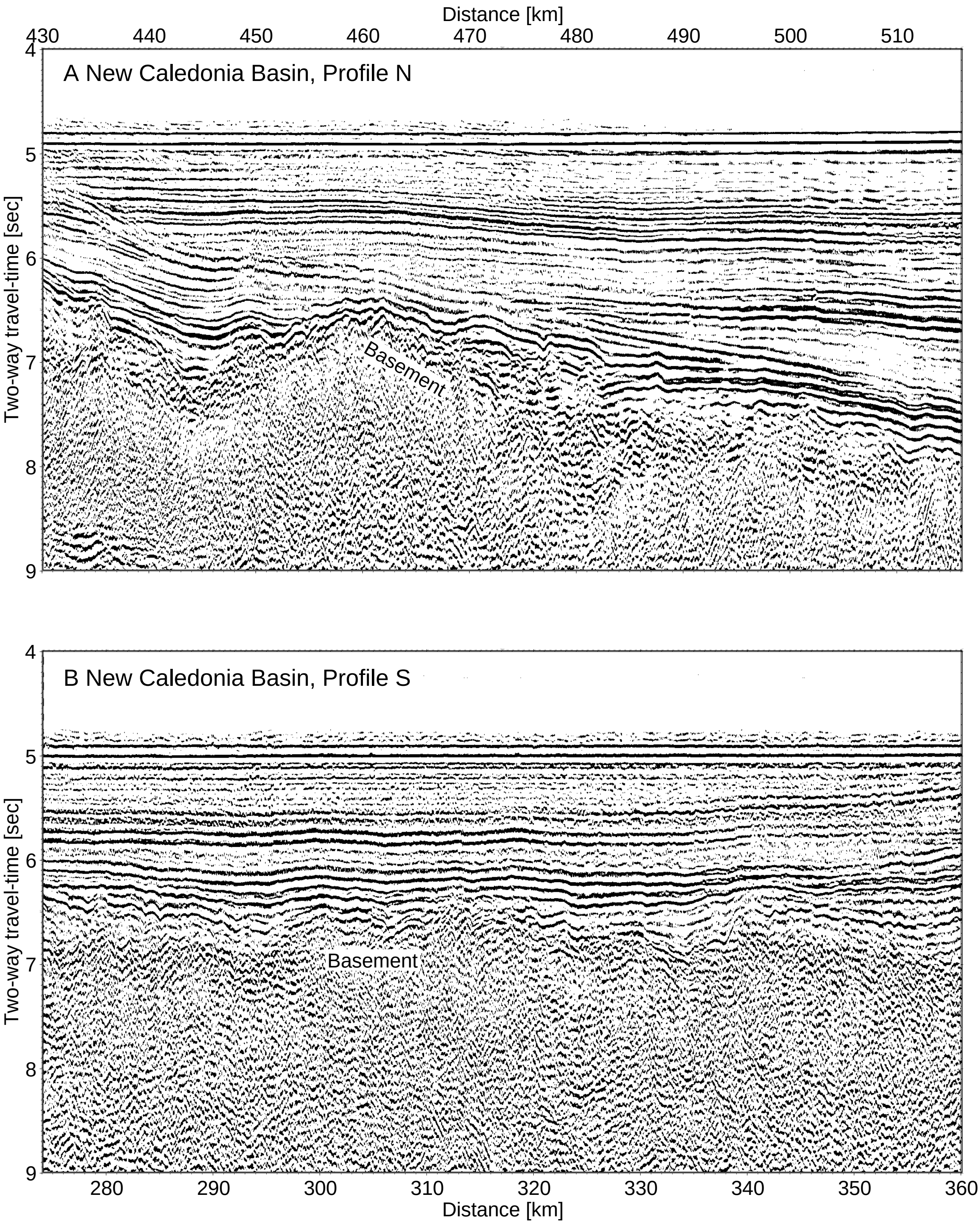
Distance [km]
430
440
450
460
470
480
490
500
510
A New Caledonia Basin, Profile N
Basement
Two-way travel-time [sec]
4
5
6
7
8
9
B New Caledonia Basin, Profile S
Basement
Two-way travel-time [sec]
280
290
300
310
320
330
340
350
360
Distance [km]

Figure 17.